Migration Letters

Volume: 21, No: S1 (2024), pp. 893-932

ISSN: 1741-8984 (Print) ISSN: 1741-8992 (Online)

www.migrationletters.com

Investigation Of Machinability Characteristics Of Sae Ams4413b Aluminum Alloy Using Ethylene Glycol As A Coolant

Roopa K. Rao[1]*, Sachin C. Kulkarni[1], Shivakumar S[1]

ABSTRACT

To understand the efficient machining of aerospace materials and achieve high quality machining, the application of coolants is essential and is based on the several factors including the types of machining process, workpiece material, tool nose radius, coolant concentration and cost. With the right type of coolants used, the performance of machining applications and the attributes of responses such as Surface roughness can be remarkably enhanced and HAZ can be improved. An attempt is made here to study the machinability and optimize the process parameters.

This paper presents an outline to optimize the Machinability studies on SAE AMS4413B alloy using Ethylene glycol as a coolant. The input parameters selected such as Cutting speed, Feed, depth of cut, coolant concentration, tool nose radius on Surface Roughness (Ra) and Heat Affected Zone (HAZ). A robust DOE based technique stresses for study of response variation using Central Composite design (CCD). The CCD design is a class of Response Surface Methodology used to design the matrix. The experiments are conducted for the confidence levels of 95%. R^2 predicted for Ra and HAZ is 95.26% and 95.51% respectively. As per the experimental analysis it is evident the individual effect of Cutting Speed, Feed, Depth of cut, Tool nose radius and Coolant concentration exists for the Ra and HAZ values. Optimum values of Ra and HAZ are 0.21 µm and 20.3 IACS. Selection of the Coolant concentration For Ethylene Glycol shall be in the range of 8-10%.

***Keywords**: Aluminum Lihium alloy - SAE AMS4413B, Ethylene Glycol, Central Composite Design (CCD) - Response surface methodology (RSM), Surface Roughness (Ra), Heat affected Zone (HAZ)*

1. INTRODUCTION

Lightweight materials play a prominent role in the aerospace industry, a sector that has been a pioneer in adopting innovative materials and production technologies. Approximately four decades ago, aluminum emerged as a dominant material in aerospace, constituting up to 70% of an aircraft [1]. [1]Over time, the aerospace and space industry has been a catalyst for the development of new material systems and manufacturing methods. The primary drivers for these advancements include the imperative to reduce weight, enhance application-specific performance, and minimize costs [2]. The historical shift from wood to aluminum alloys as the main frame material dates back to the early 1920s [3]. The appeal of aluminum lies in its cost-effectiveness, lightweight nature, ability to attain high strength levels, and ease of fabrication. This unique combination makes aluminum alloys an attractive choice, with their cost-efficiency

---

[1]Department of Mechanical Engineering, K. L. S. Gogte Institute of Technology, 590008, and Visvesvaraya Technological University, Belagavi, 590018, India.

[*]Corresponding author

often directly linked to their ease of fabrication [3]

The initial development of Al–Li alloys can be traced back to research initiatives conducted by both the United States and the Soviet Union during the Cold War era. A notable outcome of these programs was the creation of the AA2020 alloy, patented by Alcoa in 1958 [4]. Thomas Dorian [5] highlighted the features of third-generation alloys, aligning with contemporary trends in transportation industries, especially aerospace, which emphasize enhancing performance, fuel efficiency, system lifespan, and environmental sustainability to create added value. The Pioneer Aviation companies like Airbus, Lockheed, Martin, Mikayan, Gurevich and Tupolev and others are aiming for the better improved technology under the lightweight materials. Considering their strength and density (Fig 1) it becomes quite obvious why aluminum and titanium alloys are the classical lightweight aerospace alloys.

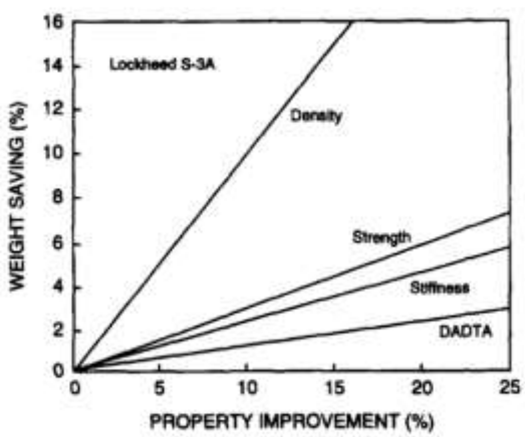

Fig 1: Graph weight savings and property improvement. [6]

Al Li alloys of third generation used for aviation applications as shown in the below Table.1 [7]. Alloys 2195, 2196, 2297, 2397, 2198, 2099, 2199, 2050, 2060, and C99N were researched and developed for space and aircraft applications, and they are referred to as 3rd-generation Al-Li Products [8]. The next generation Al–Li alloys offers better weight savings less expensive to manufacture, operate and repair. The improved material properties improved damage tolerance performance. Al–Li alloys offer improvements in the fracture processes [9-10].

Table.1: Chemical Composition of Al-Li alloys [11]

Al Li alloys	**Li**	**Cu**	**Zn**	**Mg**	**Mn**	**Fe**	**Si**	**Cr**	**Zr**	**Ti**	**Others**
2050	**0.7-1.3**	3.2-3.9	0.25	0.2-0.6	0.2-0.5	0.1	0.08	0.05	0.06-0.14	0.1	0.2-0.7 Ag
2090	**1.9-2.6**	2.4-30.0	0.1	0.25	0.05	0.12	0.1	0.05	0.08-0.15	0.15	
2098	**0.8-1.3**	3.2-3.8	0.35	0.25-0.8	0.35	0.15	0.12		0.04-0.18	0.1	0.25-0.6 Ag
2099	**1.6-**	2.4-	0.4-	0.1-	0.1-	0.07	0.0	0.1-	0.05-	0.1	0.000

	2.0	3.0	1.0	0.5	0.5		5	0.5	0.12		1 Be
2199	**1.4-1.8**	2.0-2.9	2.0-0.9	0.05-0.4	0.1-0.5	0.07	0.05		0.05-0.12	0.1	0.0001 Be

Machining is an essential part of any manufacturing industry to achieve desired components with accurate shape, size and surface finish through adequate cooling and lubrication [12]. Aluminum being an essential material being used in aerospace requirements [13]. The machining of Light weight alloys has been significant in recent years [14-27]. Study of coolants during machining to improve the surface finish and HAZ will be required for establishing the results and analysis of effect of machining parameters. Therefore, there is a need to implement sustainable cooling/lubrication system improves the machinability of light weight alloys [26]. The application of coolants is based on the several factors including the types of machining process, work-piece material, cutting tool and cost [27]. Many authors have represented their work using the various cooling lubrication method. In brief the different available cooling lubrication methods. Fig 2 Represents the possible cooling/lubrication strategies.

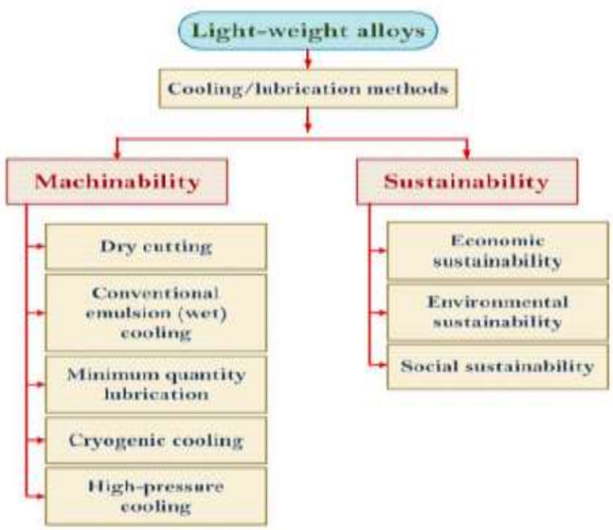

Fig 2: Coolant strategies and methods for light weight alloys [28].

2. LITERATURE REVIEW

The literature review deals with 2nd generation aluminum alloys as shown in Table 2 [29-41]. Various authors have presented the study of machinability characteristics on Al 7075 alloys. The responses evaluated suggest the use of cooling strategies, over Surface roughness, cutting force, temperature, chip morphology, etc. The authors [42-48] gave the scope on 3rd generation aluminum alloys shown in Table 3. Various authors discussed the machinability studies using the cooling strategies, for the responses such as the Surface Roughness, chip morphology, etc. Table 4. Represents the authors [49-53] having stated the use of ethylene glycol as a coolant for machinability studies.

A lot of experimental work have been done on 2nd generation materials. From the literature review, in the field of 3rd generation materials, responses of Surface roughness and Heat affected Zone using ethylene glycol as a coolant is still in experimental stage. In this investigation, DOE based RSM technique is employed to assess the output parameters. The conventional wet cooling has been used for machining of 3rd generation alloys to study the machinability characteristics of SAE AMS4413B.

Table 2: 7075 Aluminum Alloy 2nd generation material

Ref.	Workpiece	Cutting Environment	Machining	Parameters evaluated Responses	Remarks
31	AA7075	Dry, MQL Cryogenic	Turning	CF, Cutting Temperature, chip Morphology, Tool Wear	• Feed component affected by cooling techniques. • MQL and cryogenic led to lower temperature • Cooling techniques affected the lesser Tool wear
32	AA 7075-T6	Dry, MQL HPAJ, Cryogenic (LN2)(air, and vegetable oil emulsion)	Turning	Microstructure, Surface Roughness	• Analytical model for fatigue life prediction • cryogenic technique led to lower temperature
33	Al7075	Dry and Cutting fluid using Gate ECM 1	Drilling	Tool wear, Burr Measurement	• Cutting fluid resulted in lower tool wear • Cutting fluid resulted in 20%lower burr rate
34	Al 7075	Dry	Turning	MRR, SR, Cylindricity error, circularity error	• Optimization of multiple outputs • Increase in speed increased the CF also increase in SR and Circularity and cylindricity
35	Al 7075	Dry	Milling	Temperature,	• Behavior of different tool geometries and coatings
36	AA 7075	Dry, wet and cryogenic	Boring	SR, Temperature, Force	• Cryogenic leads to less Cutting force, temperature, Surface roughness • Direct application of coolant recommended
37	Al 7075 – T6	Dry, MQL, Cryogenic and Compressed air	Turning	Tool wear, SR, Micro hardness, Force, Chip Morphology	• MQL, RHVT, and Compressed air, for improvement in SR and Tool wear • Absence of Crater wear due to coolant conditions
38	Al 7075 – T6	Coolant not specified	Milling	SR,	• Nose radius and depth of cut significant for minimizing the Surface roughness
39	Al 7075	Wet and LN2	Turning	SR, Temperature, Force	• Use of LN2 reduced the temperature, forces and surface roughness •

40	Al 7075	MQL, Compressed Air	Milling	SR, MRR	• Speed and Feed rate was the important parameter that affected the SR • Less viscous the coolant is effective
41	Al 7075 – T6	Dry and MQL using Mecgreen 550 Lubricant	Turning	SR and Chip formation	• Chip formation is dependent on feed rate, CS and Lubricating conditions • SR mainly dependent on feed rate
42	Al 7136-T6511	Blastocut BC 35 SW	Milling	SR	• CS is the factor that Affects the SR.
43	Al 7075-T6	Nano Silver and Borax additives with 95% ethylene glycol (Suspension form)	Milling	SR, CF and Chip formation	• Tribological Performance of Borax and nano Silver added EG • Nano Silver particles will improve the SR and solution prepared with EG has an industrial usage.

Table 3: 3rd Generation Aluminum alloys

Ref.	**Workpiece /Tool material**	**Cutting Environment**	**Machining**	**Parameters evaluated Responses**	**Remarks**
44	AA2024-T3	Dry, Base Fluid (Mineral Oil) MQL, NFMQL MoS2	Turning	Surface Topography, Temperature	• Surface Roughness was better with NFMQL than dry and MQL because of MoS2 • BUE is less with NFMQL
45	AA2050	Soluble oil emulsion	Tapping	Machining Distortion MRR	• Optimization of Machining time • Low values of distortion from the geometrical tolerances
46	Al2050	Dry and WET Emulsion Quakercool 7000 ALF 8%	Milling	Chip Morphology	• CS assists in reducing the chip size • Reduction in rake angle reduces the chip thickness

47	2A 97	Dry	Milling	Chip Morphology, Ra	• Cutting Speed played an important role for chip edge • Convenient for replacing the Conventional Al alloys for aircrafts
48	Al 8112	Vegetable oil (Copra Oil) as base oil, nano fluid	Milling	MRR	• Increase in depth of cut increases the MRR • Helix angle plays an important role for improving the MRR
49	Aluminium alloy 24345	Dry	Milling	Ra and Rz	• Uncoated and polished flute cutters perform far better coated cutters • Rz and Sdr give a better picture of the actual surface from the functionality point of view
50	Al 2024-T3	Dry	Drilling	Hole Deviation and Circularity	• Burrs were less with uncoated drill bit • CS also the significant parameter for geometrical parameters

Table 4: Coolant as Ethylene Glycol

Ref.	**Workpiece**	**Cutting Environment**	**Machining**	**Parameters evaluated Responses**	**Remarks**
51	SUS 304	Cellulose nanocrystal ethylene glycol	Turning	Thermal Conductivity Analysis, cutting tool and chp thermal analysis,	• Thermal conductivity increases as concentration increases
52	AISI 1018	Ethylene glycol as base fluid, TiO2 and Al2O3 nanoparticles	Turning	Temperature, SR	• Thermal Analysis was studied along with SR
	Al 3303	Water ethylene glycol mixture		Corrosion study	• Corosion properties

53	AISI 304	Ethylene glycol TiO2 nano particles	Milling	Tool life, tool wear	• Tool ife decreases with increase increase in cutting speed • Showed better performance with water soluble coolants in terms of tool life.
54	AA6061-T6	Ethylene glycol mixture with TiO2 and ZnO hybrid nano coolant	Milling	SR, MRR	• Suitable alternative and compatible in using the hybrid nano-coolant
55	Fe3O4 nanofluid	Ehtylene glycol and waterbased mixture		Thermal Conductivity, Effect of temperture	• Thermal Conductivity enhancement

3. EXPERIMENTAL SETUP

All the machining has been carried out on an DMG MORI 3 Axis CNC milling machine. Machining was undertaken using three varying cutting parameters: cutting speed, feed rate and depth of cut. and coolant concentration with 8%, 10% and 12%. Suitable combinations of the cutting parameters were used to deduce the design of the experiment using the CCD method with three factors five levels Table 5. A total of 156 combinations of experiments were undertaken. The process parameters are as in the below table [57] The Milling was carried out with 100% engagement of 30 x 30 mm on the specimen. Aluminum Lithium alloy SAE AMS4413B slabs are used for experimentation. The size of each block was 50 x 50 x 20 mm as shown in the Fig 3. The chemical composition of the work piece material and the properties of the work piece material are shown in Table 6 and Table 7. The milling inserts (Fig. 4) by SECO Uncoated tools signature [59]. The uncoated insert is XOEX10T304 standard water-soluble Ethylene glycol coolant was used as the flood coolant as shown in Table 8.

Table 5: Process parameters

Variables			**Levels**	
		-1	**0**	**1**
Cutting Speed(rpm)	X1	5000	11000	17000
Feed(mm/tooth)	X2	0.04	0.16	0.28
Depth of Cut(mm)	X3	0.5	1	1.5
Tool Nose Radius	X4	0.4	0.8	1.2
Coolant Concentration (%)	X5	8	10	12

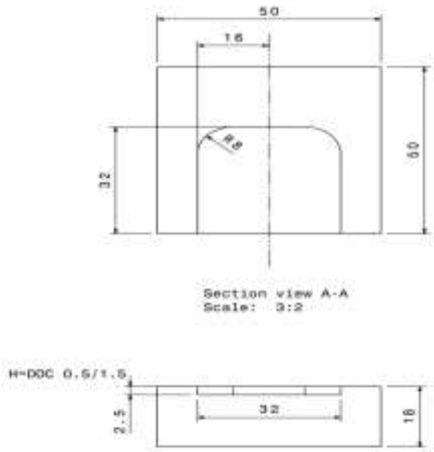

Fig 3: Sample specimen drawing of size 50 x 50 x 20 mm

Table 6: Chemical composition of workpiece material.

Cu	Li	Mg	Mn	Ag	Zr	Bal.
3.5	0.9	0.40	0.35	0.45	0.12	Re m.
SAE AMS4413B Solution Heat Treated, Stress Relieved, and Artificially Aged						

Table 7: Physical properties of 3rd Generation

Properties	Value
Density	270 gm/cc
Melting point	510 ° C
Tensile Strength	440 MPa
Yield Strength	370 MPa
Shear Strength	260 MPa
Fatigue Strength	125
Elastic Modulus	70-80 GPa
Poison’s Ratio	0.33
Elongation	10%

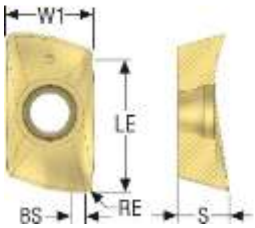

Fig 4: Seco Insert Carbide Uncoated from XOEX10T3

Table. 8: Coolant Details: Specifications of Ethylene Glycol: MOLYCHEM

Ethylene Glycol	1,2 Ethanediol
Ethylene Glycol	98%
Molecular formula	C2H6O2
Color	A clear colorless, slightly viscous liquid
Wt. per ML at 20°C	1.112-1.115g

3.1 PERFORMANCE EVALUATION:

Surface roughness and surface finish are opposite to each other, these are quantitative parameters. Surface roughness can be expressed in units of length after its measurement. "Measurement of finely spaced deviations of actual surface from nominal surface (datum) in the units of length (µm) is the measurement of surface roughness. Lesser the value of surface roughness better the surface finish is said. There are two popular methods of expressing measured value of surface roughness.

According to "AA" method surface roughness is the average of vertical deviations from the nominal surface over a specified surface length.

Average roughness (AA)

$$= \int_0^{lm} \frac{(Y)}{Lm} dx$$

Heat Affected Zone: Eddy current meter has been used to measure the HAZ. Portable meter with specifications High resolution color display and Accurate conductivity range: 0.5% IACS to 110% IACS, 0.28-64Ms/m, Digital Temperature readout The following pictures represent the experimental setup and testing done.

Fig: 5: Specimen Before machining

Fig. 6: Secimen After Machining

Fig. 7: Experimental set-up of the milling of a sample specimen

Surface roughness measurement using 410 Surf test on Sample specimen

HAZ measurment using Eddy current meter on Sample specimen

Fig 8: Testing of Ra and HAZ using 410 Surf-test and EDDY current meter

4. RESULTS AND DISCUSSION

In order to measure the statistical significance, analysis of variance (ANOVA) is used and

results for the Ra, and HAZ are tabulated in Table 9 and Table 10 respectively. The Results of interaction plots are placed.
The Regression equation of the analysis for Ra and Surface Roughness obtained is mentioned below:

Ra = 5.605 + 5.32 X2 - 1.674 X4 – 9.02 $X2^2$ + 0.0387 $X5^2$ + 0.000077 X1 * X5 - 2.573 X2 *X4 + 0.3649 X2 *X5 - 0.0865 X3 *X4 + 0.1102 X4 *X5

HAZ = 24.511 - 0.2131 X3 - 1.599 X4 – 0.582 X5 - 0.0909 $X3^2$ + 0.583 $X4^2$ + 0.02311 $X5^2$ - 0.000063 X1 * X3 + 0.000117 X1*X4 - 0.000049 X1 * X5 +1.258 X2 *X4 + 0.1430 X2 *X5 - 0.0788 X3 *X4 + 0.03185 X3 *X5 + 0.07090 X4 *X5

Source Ra	**Un-Coded Values**	**DF**	**Adj SS**	**Adj MS F-Value**	**F-Value**	**P value**	**Significant Factors**
Model		20	37.69580	1.88480	13.70000	0.00000	
Linear		5	33.27930	6.65590	479.20000	0.00000	
Cutting Speed	X1	1	0.06440	0.06440	4.63000	0.13800	
Feed	X2	1	31.11960	31.11960	2240.51000	0.00000	*
Depth of Cut	X3	1	0.00880	0.00880	0.63000	0.35800	
Tool Nose Radius	X4	1	1.26500	1.26500	91.07000	0.00000	*
Coolant Concentration	X5	1	0.82170	0.82170	59.16000	0.67600	
Square		5	1.00750	0.20150	14.51000	0.00000	*
Cutting Speed * Cutting Speed	$X1^2$	1	0.02450	0.02450	1.76000	0.18600	
Feed * Feed	$X2^2$	1	0.12530	0.12530	0.02000	0.00300	*
DOC * DOC	$X3^2$	1	0.00000	0.00000	0.00000	0.99900	
Tool Nose radius*Tool Nose radius	$X4^2$	1	0.04020	0.04020	2.90000	0.09100	
Coolant Concentration*Coolant Concentration	$X5^3$	1	0.17500	0.17750	12.78000	0.00000	*
2-Way Interaction		10	3.40900	0.34090	24.54000	0.00000	
Cutting Speed*Feed	X1 * X2	1	0.01360	0.01360	0.98000	0.32400	

Cutting Speed*Depth of Cut	X1 * X3	1	0.0052 0	0.0052 0	0.38000	0.5410 0	
Cutting Speed*Tool Nose radius	X1 * X4	1	0.0370 0	0.0370 0	2.66000	0.1050 0	
Cutting Speed*Coolant Concentration	X1 * X5	1	0.2031 0	0.0203 1	14.63000	0.0000 0	*
Feed*Depth of Cut	X2 * X3	1	0.0878 0	0.0878 0	6.32000	0.0130 0	
Feed*Tool Nose radius	X2 * X4	1	1.4642 0	1.4642 0	105.4200 0	0.0000 0	*
Feed*Coolant Concentration	X2 * X5	1	0.7364 0	0.7364 0	53.02000	0.0000 0	*
Depth of Cut*Tool Nose radius	X3 * X4	1	0.1150 0	0.1150 0	8.28000	0.0000 0	*
Depth of Cut*Coolant Concentration	X3 * X5	1	0.0000 0	0.0000 0	0.00000	0.9600 0	
Tool Nose radius*Coolant Concentration	X4 * X5	1	0.7466 0	0.7466 0	53.75000	0.0000 0	*

Table 9: ANOVA (Ra)

Table 10: ANOVA (HAZ)

Source HAZ	**Un-Coded Values**	**DF**	**Adj SS**	**Adj MS F-Value**	**F-Value**	**P value**	**Significant Factors**
Model		20	9.62100	0.48060	143.51000	0.00000	
Linear		5	7.87910	1.57583	470.55000	0.00000	
Cutting Speed	X1	1	0.04055	0.10547	31.50000	0.00000	
Feed	X2	1	0.02100	0.02104	6.28000	0.01300	*
Depth of Cut	X3	1	6.93690	6.93686	2071.40000	0.00000	
Tool Nose Radius	X4	1	0.62510	0.62510	186.66000	0.00000	*
Coolant Concentration	X5	1	0.19070	0.19067	56.93000	0.00000	*
Square		5	0.33000	0.06739	20.12000	0.00000	*
Cutting Speed * Cutting Speed	$X1^2$	1	0.00230	0.00229	0.68000	0.40900	
Feed * Feed	$X2^2$	1	0.00000	0.00002	0.01000	0.94000	*
DOC * DOC	$X3^2$	1	0.06140	0.06137	18.33000	0.00000	*
Tool Nose radius*Tool Nose radius	$X4^2$	1	0.06460	0.06460	19.29000	0.00000	*
Coolant Concentration*Coolant Concentration	$X5^3$	1	0.06350	0.06345	18.95000	0.00000	*
2-Way Interaction		10	1.39600	0.13960	41.68000	0.00000	*
Cutting Speed*Feed	X1 * X2	1	0.00140	0.00139	0.41000	0.52100	
Cutting Speed*Depth of Cut	X1 * X3	1	0.03470	0.03469	10.36000	0.00200	*
Cutting Speed*Tool Nose radius	X1 * X4	1	0.01880	0.01884	5.63000	0.01900	
Cutting Speed*Coolant	X1 * X5	1	0.08140	0.08138	24.30000	0.00000	*

Concentration							
Feed*Depth of Cut	X2*X3	1	0.00310	0.00309	0.92000	0.33800	
Feed*Tool Nose radius	X2*X4	1	0.34980	0.34981	104.46000	0.00000	*
Feed*Coolant Concentration	X2*X5	1	0.11310	0.11309	104.46000	0.00000	*
Depth of Cut*Tool Nose radius	X3*X4	1	0.11310	0.11309	33.77000	0.00000	*
Depth of Cut*Coolant Concentration	X3*X5	1	0.38950	0.38951	116.31000	0.00000	*
Tool Nose radius*Coolant Concentration	X4*X5	1	0.30880	0.30883	92.22000	0.00000	*

Interaction plots for Ra

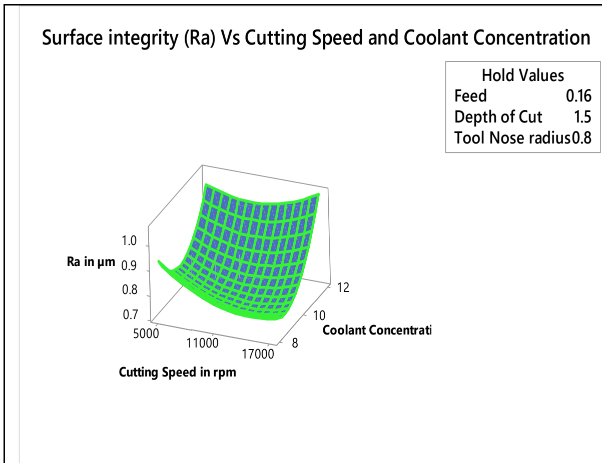

4.1 a.

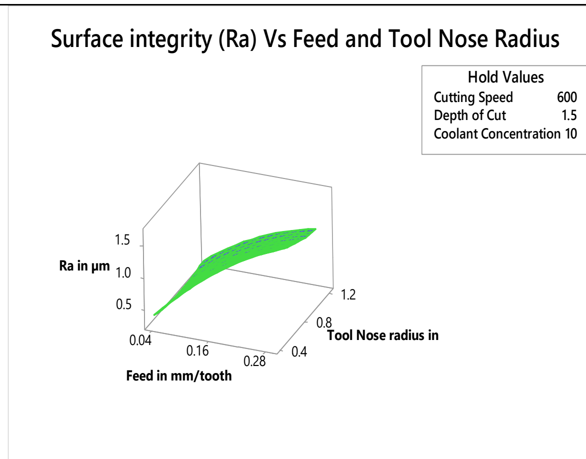

4.1.b

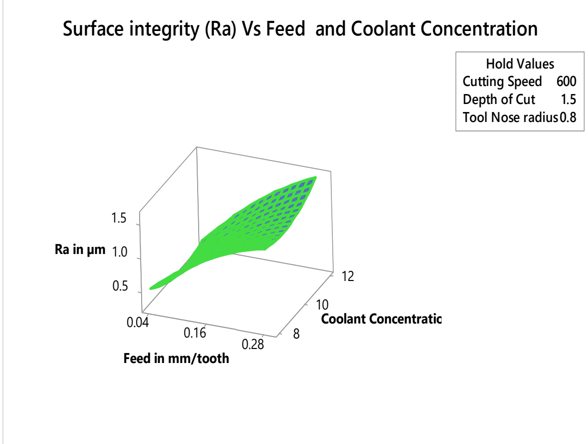

4.1.c

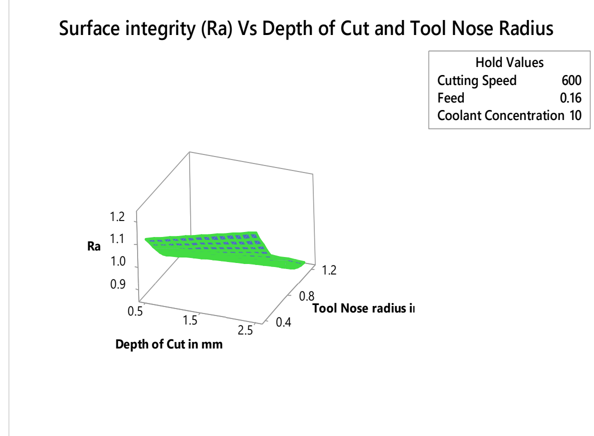

4.1.d

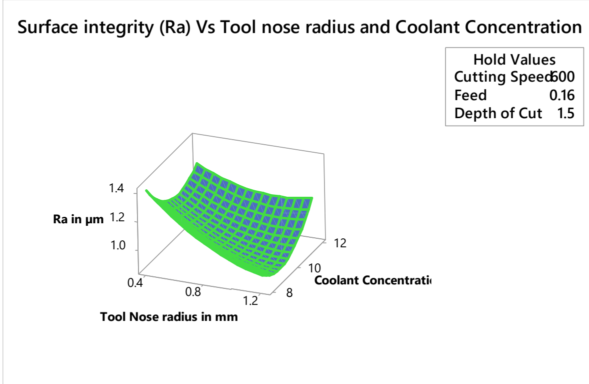

4.1.e

Fig: 4.1 a) Surface plot of CS and Coolant connetration b) Surface plot of Feed and Tool nose radius c) Surface plot of Feed and Coolant connetration d) Surface plot of Depth of Cut and Tool nose radius e) Surface plot of Tool nose radius and Coolant connetration

Fig: 4.1.a-4.1.e shows the Surface plots when Ethylene glycol being used as the coolant with 8%, 10% and 12% concentration. The figures represent the effect of input parameters on the Surface Roughness (Ra). The Surface plots 4.1.a indicates the sudden decrease and increasing trend for cutting speed and coolant concentration. Whereas fig: 4.1.b and 4.1.c indicates the increasing trend for interaction between feed and coolant concentration as well as tool nose radius. The interaction plot 6.d indicates Tool nose radius and depth of cut a decreasing trend of Ra value. The Fig: 4.1.e shows a decreasing trend indicating higher value of tool nose radius and coolant concentration of 8-10%.

Contour plots for Ra

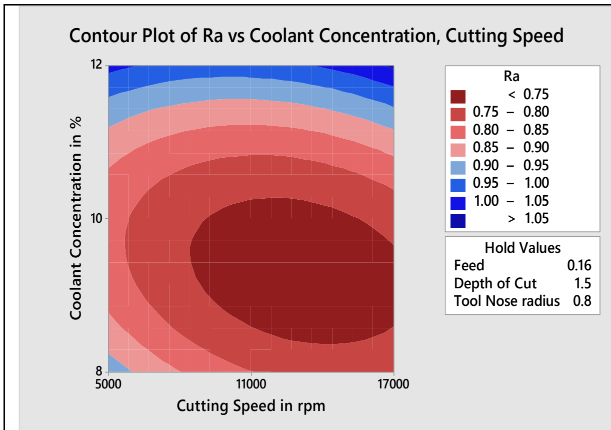

4.2.a

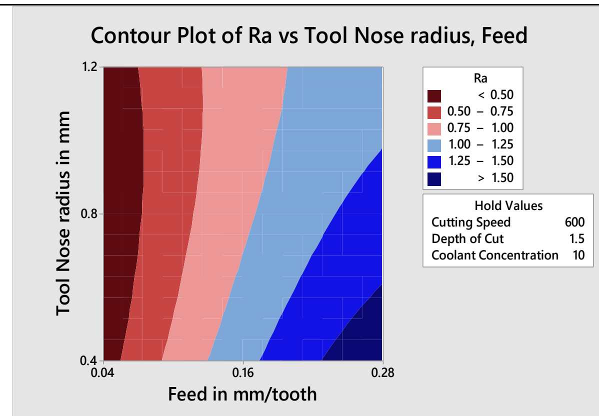

4.2.b Contour plots for Feed and Tool nose radius

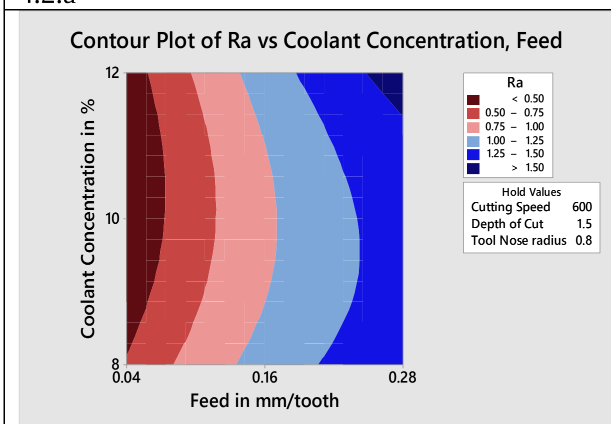

4.2.c

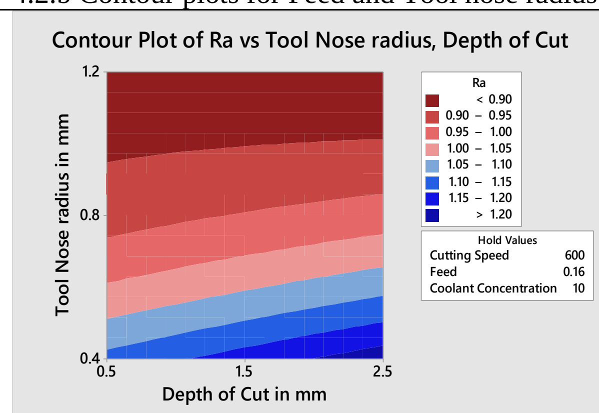

4.2.d

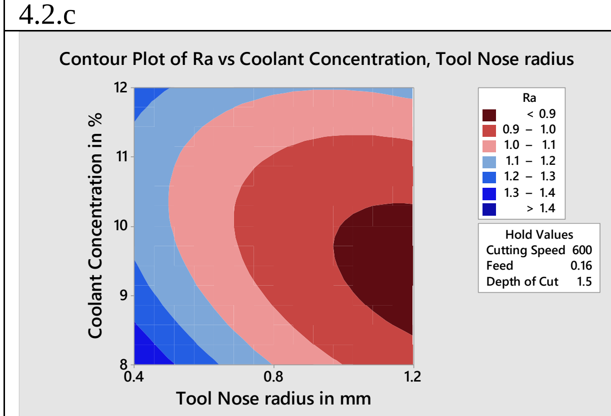

4.2.e

Fig: 4.2. a) Contour plots for Cutting speed and Coolant concentration b) Contour plots for Feed and Tool nose radius c) Contour plots for Feed and Coolant concentration d) Contour plots for Depth of cut and Tool Nose radius e) Contour plots for Coolant concentration and Tool nose radius

Fig 4.2.a – 4.2.e represents the contour plots for interaction between cutting speed, feed, depth of cut, tool nose radius and coolant concentration on Surface Roughness (Ra). The Fig 4.2.a shows the Simple maximum pattern of the contour plot for the hold values of speed 11000 rpm, 0.16 mm/tooth feed and Depth of cut of 1.5mm with Ra values less than 0.75µm. Fig: 4.2.b - 4.2.d represents the stationary ridge pattern and 4.2.e the rising ridge pattern on the contour plot with Ra values less than 0.50 µm, 0.90 µm respectively withhold values of speed 11000 rpm, 0.16 mm/tooth feed and Depth of cut of 1.5mm. From the above surface and contour plots it is observed that cutting speed between 11000 rpm and 17000 rpm can be considered with lower feed of 0.04 mm/tooth and larger tool nose radius and coolant concentration.

Interaction plot for HAZ

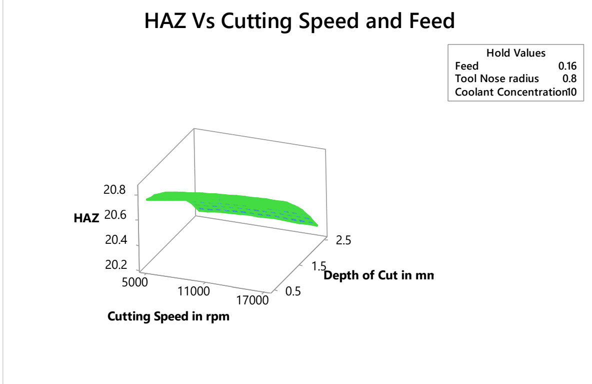

4.3.a

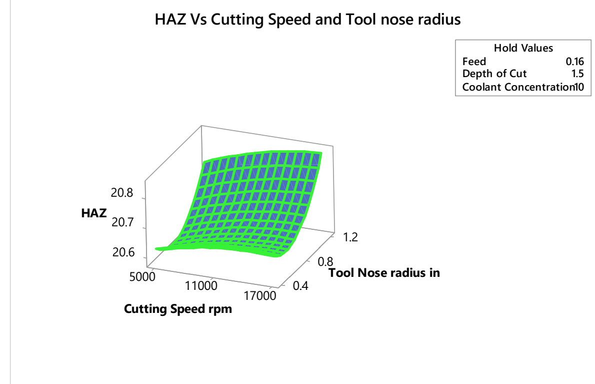

4.3.b

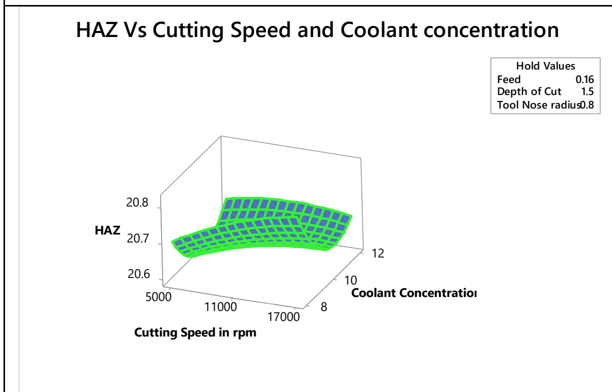

4.3.c

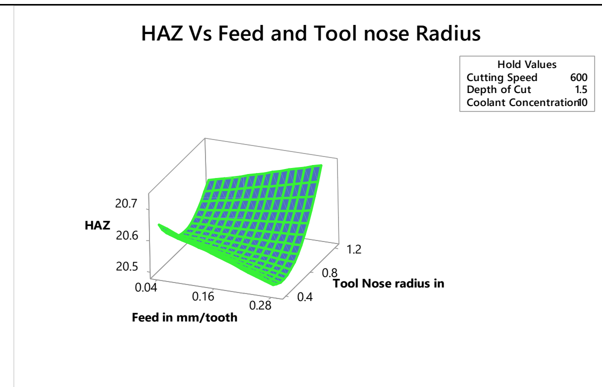

4.3.d

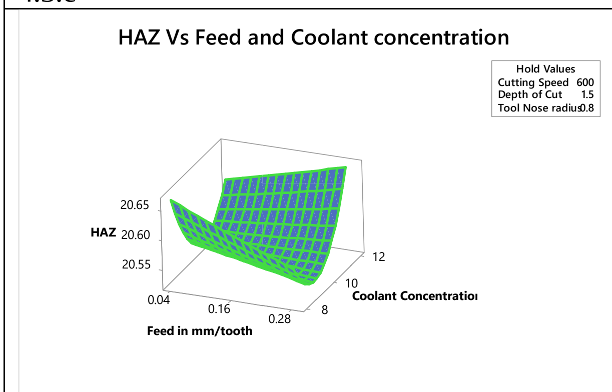

4.3.e

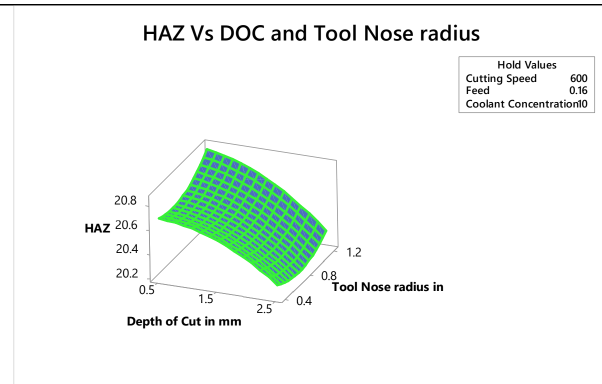

4.3.f

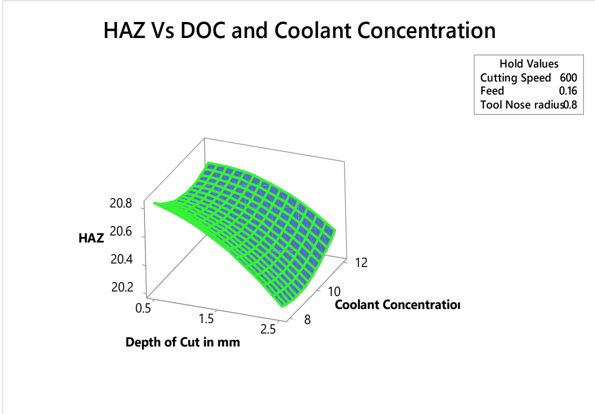

4.3.g

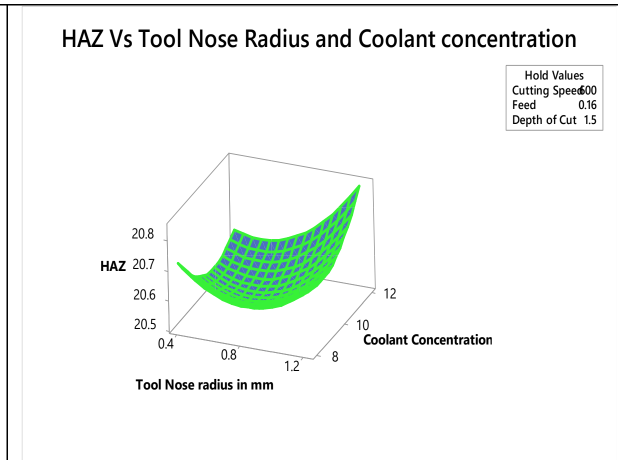

4.3.h

Fig: 4.3.a) Surface plot of Cutting speed and depth of cut, b) Surface plot of Cutting speed and tool nose radius, c) Surface plot of CS and Coolant concentration, d) Surface plot of Feed and Tool nose radius, e) : Interaction plot: Surface plot of CS and Coolant connetration, f) Surface plot of Feed and Tool nose radius, g) Surface plot of Depth of cut and Coolant connetration, h) Surface plot of Coolant concentration and Tool nose radius

Fig: 4.3.a-4.3.e represents the Surface plots for Heat affected zone. The hold values for all the plots is with Cutting Speed as 11000 rpm, Depth of cut 1.5 mm, Tool nose radius as 0.8mm and 0.16 mm/tooth feed and 10% coolant concentration. Fig.6.a indicates a better lubrication since for all the speed values the HAZ is showing a decreasing trend for increasing Depth of cut. Fig. 4.b, indicates that the lower HAZ can be obtained by employing 0.4 mm tool nose radius with 10% coolant concentration. Fig 4.c shows sudden decrease and then increase in the HAZ for interaction between cutting speed and coolant concentration. Fig 3.d and 3.e indicates lower values of HAZ for cutting speed of 17000 rpm, lower feed and smaller tool nose radius along with 8%-10% coolant concentration. Fig.4.f and 4.g indicates that the Lower values of HAZ can be obtained with coolant concentration of 10% for dept of cut up to 2.5 mm. Fig. 4.6.h Shows lower HAZ for Tool nose radius as 0.8mm and 10% coolant concentration. From the surface plots up to 10% of coolant concentration and tool nose radius of 0.4-0.8 mm can be employed.

Contour Plots for HAZ

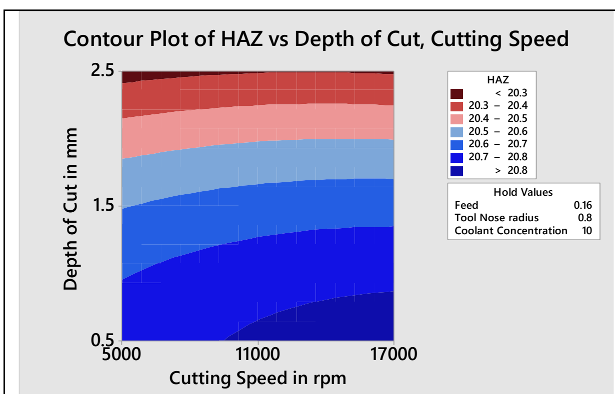

4.4.a

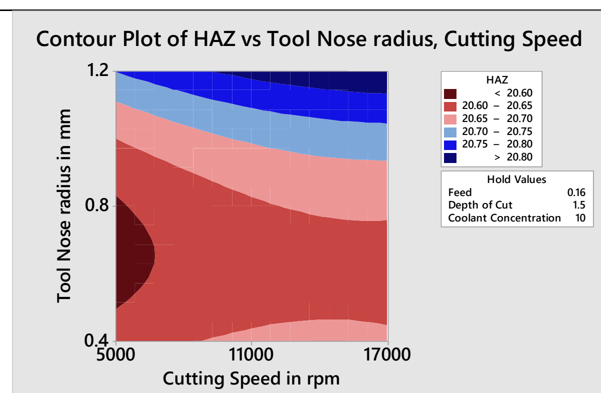

4.4.b

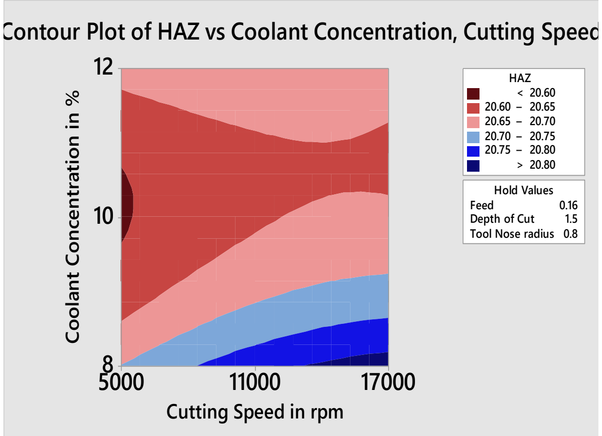

4.4.c

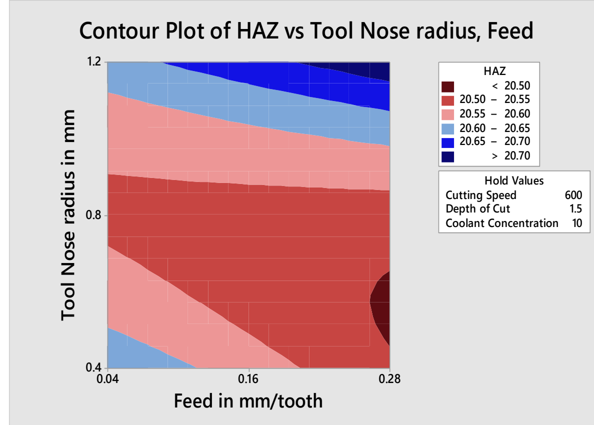

4.4.d

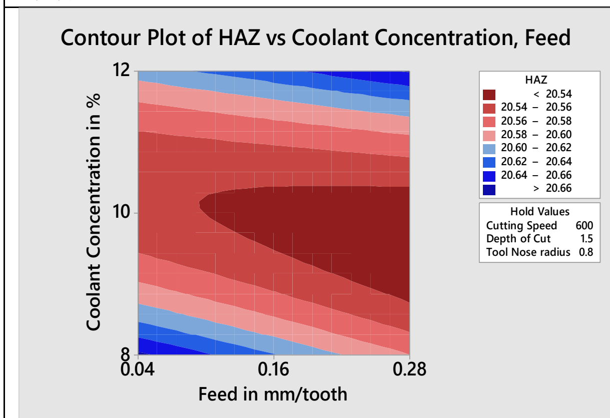

4.4.e

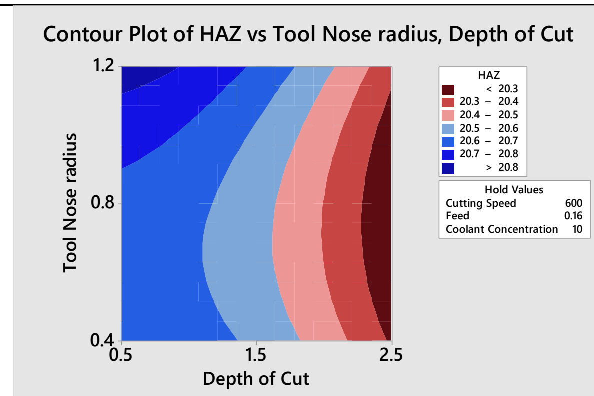

4.4.f

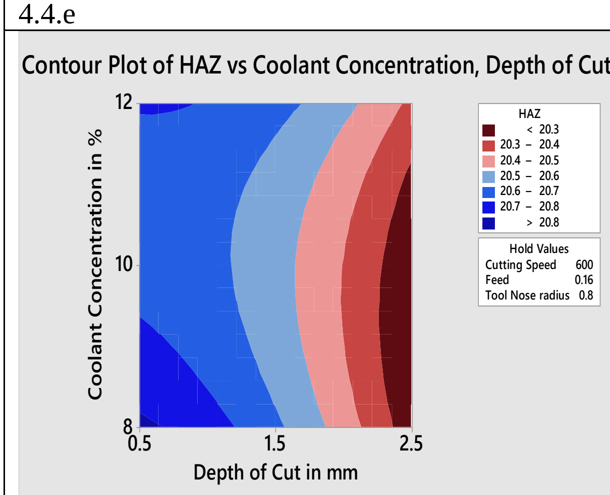

4.4. g

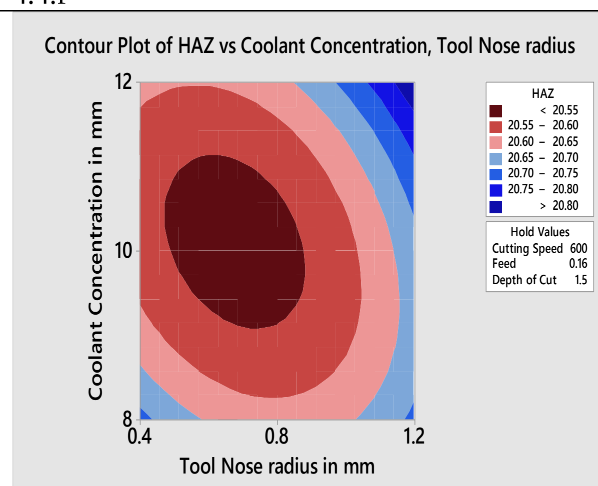

4.4.h

4.4.a) Contour plots for Cutting speed and Depth of Cut, b) Contour plots for Cutting Speed and Tool nose radius, c) Contour plots for Cutting speed and Coolant concentration, d) Contour plots for Feed and Tool nose radius, e) Contour plots for Feed and Coolant concentration, f) Contour plots for Depth of Cut and Tool nose radius, g) Contour plots for Depth of cut and Coolant concentration, h) Contour plots for Coolant concentration and Tool nose radius

Fig 4.4.a – 4.4.h represents the contour plots for interaction between cutting speed, feed, depth of cut, tool nose radius and coolant concentration on Heat affected zone (HAZ). Fig.4.4.a indicates the stationary ridge pattern with HAZ values less than 20.3 IACS. Fig.4.4.f-4.4.g shows the minimax pattern of the contour plot for the hold values of speed 11000 rpm, 0.16 mm/tooth feed and Depth of cut of 1.5mm with HAZ values of 20. IACS. Fig: 3.4. b, c, d represents the stationary ridge pattern and 4.4.e the rising ridge pattern on the contour plot with HAZ values lesser than 20.5 and 20.6 IACS respectively withhold values of speed 11000 rpm, 0.16 mm/tooth feed and Depth of cut of 1.5mm. Fig 3.4.e indicates that the rising ridge pattern with HAZ 20.55 IACS value

5. CONCLUSION

Based on the experimental work the following conclusions were drawn:

The individual effect of Cutting Speed, Feed, Depth of cut, Tool nose radius and Coolant concentration exists for the Ra and HAZ values. Optimum values of Ra and HAZ are 0.21 µm and 20.3 IACS. Selection of the Coolant concentration For Ethylene Glycol shall be in the range of 8-10%. The Linear model Analysis are well within the 95 % confidence level with R2 as 95.27 % for Ra values and 95.51 % for HAZ respectively. The experimental results shall be a scope for researchers.

5. ACKNOWLEDGEMENT

We acknowledge Aequs Pvt Ltd. for providing the infrastructure for conduction of experiments and Kulkarni Precitech Pvt Ltd. for providing the facility for specimen preparation and pilot reading. All experiments were conducted under the safe supervision of guide and experts at Industry.

Conflicts of interest: There are no conflicts of interest.

6. REFERENCES

Analysis and optimization of surface quality while machining high strength aluminium alloy", Elsevier, Measurement, Volume 152, February 2020, 107337

A M Zetty Akhtar1 , M M Rahman1,2 , K Kadirgama1,2 and M A Maleque, Effect of TiO2 and Al2O3-ethylene glycol-based nanofluids on cutting temperature and surface roughness during turning process of AISI 1018

Afaf M. Abd El-Hameed, Y. A. Abdel-Aziz, Aluminum Alloys in Space Applications: A Short Report, Journal of Advanced Research in Applied Sciences and Engineering Technology 2022, Issue 1 (2021) 1-7

Afaf M. Abd El-Hameed1, Y. A. Abdel-Aziz, Aluminium Alloys in Space Applications: A Short Report, Academia Baru , Journal of Advanced Research in Applied Sciences and Engineering Technology 22, Issue 1 (2021) 1-7

Aishah Najiah Dahnel, Muhamad Ali Abdul Ghani, Natasha A. Raof, Suhaily Mokhtar , and Nor Khairusshima Muhamad Khairussaleh, Analysis of defects on machined surfaces of aluminum alloy (Al 7075) using imaging and topographical techniques, International Journal of Metrology and Quality Engineering Int. J. Metrol. Qual. Eng. 13, 12 (2022) A.N. Dahnel et al., published by EDP Sciences, https://doi.org/10.1051/ijmqe/2022012

Aleksandar Košarac, Lana Šikuljak, Čedomir, Cvijetin Mlađenović, Milan Zeljković, CUTTING PARAMETERS INFLUENCE ON SURFACE ROUGHNESS IN AL 7075 MILLING, 19th International Symposium INFOTEH-JAHORINA, 18-20 March 2020, DOI: 10.1109/INFOTEH48170.2020.9066273

and Space

Applications, METALLURGICAL AND MATERIALS TRANSACTIONS A VOLUME 43A,

SEPTEMBER 2012—3325
Arpit Srivastava1, Mukesh K, umar Verma1, Ramendra Singh Niranjan1, Abhishek Chandra1, Praveen Bhai Patel1, Experimental Investigation and Optimization of Machining Parameters in Turning of Aluminum Alloy 075-T651, Sciendo, PRODUCTION ENGINEERING ARCHIVES2021, 27(4),296-305
Atul Dev!, Smriti Tandon# , Pankaj Kumar$, and Anup Dutt, Effect of Coating and Polishing of Cutting Tool on Machined Surface Quality in Dry Machining of Aluminium Alloy, Defence Science Journal, Vol. 70, No. 3, May 2020, pp. 299-305, DOI : 10.14429/dsj.70.14831 © 2020, DESIDOC
Aurel Mihail Titu, Andrei Victor Sandu, Alina Bianca Pop, Stefan Titu, Dragos Nicolae Fratila and Costel Ceocea Design of Experiment in the Milling Process of Aluminum Alloys in the Aerospace Industry. MDPI AG Applied Sciences (Vol. 10, Issue 19)
Aysegul Yucel, Cagri vakkas yildirim, Murat Sarikaya , Senol Sirin , Turgay Kivak, Munish Kumar Gupta, Italo V . Tomaz . Influence of MoS 2 based nanofluid – MQL on tribological and machining characteristics in turning of AA 2024 T3 aluminum alloy , jmr&t Journal of Material Research and Technology , ELSEVIER JOURNAL OF MATERIALS REASEARCH AND TECHNOLOGY 2021;15 : 1688- 1704
Cindie Giummarra, Bruce Thomas and Roberto J. Rioja, New Aluminum Lithium Alloys For Aerospace Applications, Proceedings of the Light Metals Technology Conference 2007,
E. A. Starke, Jr and J. T. Staley, Application of modern aluminum alloys to Aircraft, Pro 9. Aerospace Sci. Vol. 32, pp. 131-172~ 1996 Elsevier Science Ltd Printed in Great Britain.
Elvan Ates, Zafer Evis, Fahrettin Ozturk, "Optimization of cutting parameters and machining Distortion analysis for AA2050", Metal 2022, May 18-19,2022 Brno Czech Republic, EU
F. C Campbell, Manufacturing Technology for aerospace structural materials, Elsevier, 2011
G. Ambrogio, L. Filice, F. Gagliardi, Materials and Design Materials and Design, Elsevier, 34 (2012) 501–508 Content
G. Le Coz a, M. Marinescu a, A. Devillez a, D. Dudzinski a, L. Velnom b, Measuring temperature of rotating cutting tools: Application to MQL drilling and dry milling of aerospace alloys, Applied Thermal Engineering, Elsevier, Volume 36, April 2012, Pages 434-441
G.C. Manjunath Patel, Deepak Lokare, Ganesh R Chate, Mahesh.B. Parappagoudar, R. Nikhil, Kapil Gupta,
Gary Wong Ang Kui1 · Sumaiya Islam1 · Moola Mohan Reddy1 · Neamul Khandoker2 · Vincent Lee Chieng Chen1, Recent progress and evolution of coolant usages in conventional machining methods: a comprehensive review, The International Journal of Advanced Manufacturing Technology (2022) 119:3–40,
Giovanna Roella, Effect of surface integrity induced by machining on high cycle fatigue life of 7075-T6 aluminum alloy, May 2019, Journal of Manufacturing Processes 41:83-91, 10.1016/j.jmapro.2019.03.031
Imhade Princess Okokpujie and Lagouge Kwanda Tartibu, Performance Investigation of the Effects of Nano-Additive-Lubricants with Cutting Parameters on Material Removal Rate of AL8112 Alloy for Advanced Manufacturing Application, Advanced Manufacturing Application. Sustainability , MDPI, 2021, 13, 8406. https:// doi.org/10.3390/su13158406,
Jasjeevan Singh Simranpreet Singh Gill , Turning of Al 7075-T6 aerospace alloy under different sustainable metalworking fluid strategies by coated carbide tools, Pages 275-294 Received 04 Jan 2023, Accepted 08 May 2023, Published online: 20 May 2023 Surface Engineering , Taylor and fancies Volume 39, 2023 - Issue 3
Jintao Niu, Zhanqiang Liu, Xing Ai, Weimin Huang, Guijie Wang & Ran Duan Characteristics of machined surface integrity in face milling Al-Li alloy 2A97 with carbide inserts, The International Journal of Advanced Manufacturing Technology, Springer 101, pages839–848 (2019)
K Thirumavalavan1, Sastry C Chandrasekhar1, Abeens M1, R Muruganandhan1 and M A Muthu Manickam2, Materials Research Express, Volume 6, Number 11, IOP DOI 10.1088/2053-1591/ab522f
K. Danesh Narooei 1 R. Ramli 2 Optimal Selection of Cutting Parameters for Surface Roughness in Milling Machining of AA6061-T6, IJE TRANSACTIONS C: Aspects Vol. 35, No. 06, (June 2022) 1170-1177

Kailun Zheng, Denis J. Politis, Liliang Wang, Jianguo Lin, A Review on Forming Techniques for Manufacturing Lightweight Complexed Shaped Aluminium Panel Components", International Journal of Lightweight Materials and Manufacture 1(2018) 55-80

Kamran Dehghani , Atiye Nekahi , Mohammad Ali Mohammad Mirzaie, Optimizing the bake hardening behavior of Al7075 using response surface methodology, Materials & Design

L. Syam Sundar, Manoj Kumar Singh, Antonio Sousa, Thermal conductivity of ethylene glycol and water mixture based Fe3O4 nanofluid, International Communications in Heat and Mass Transfer 49:17–24 DOI:10.1016/j.icheatmasstransfer.2013.08.026

L. Zhu, N. Li, P.R.N. Childs, "Light-weighting in aerospace component and system design", , Propulsion and Power Research 2018;7(2):103–119

L. Samylingam , K. Anamalai a, K. Kadirgama , M. Samykano , D. Ramasamy , M.M. Noor , G. Najaf i , M.M. Rahman, Hong Wei Xian , Nor Azwadi Che Sidik, Thermal analysis of cellulose nanocrystal-ethylene glycol nanofluid coolant, International Journal of Heat and Mass Transfer, Elsevier, Volume 127, Part B, December 2018, Pages 173-181

M. Huseyin Cetin, Seyma Korkmaz Investigation of the concentration rate and aggregation behaviour of nano-silver added colloidal suspensions on wear behaviour of metallic materials by using ANOVA method, Tribology International, Elsevier Volume 147, July 2020, 106273

M. Peters and C. Leyens, "Materials Science and Engineering – Vol. III – Aerospace and Space Materials, Encyclopedia of Life Support Systems (EOLSS)

Michael Standridge, Aerospace materials past, present, and future", aerospacemanufacturinganddesign.com/article/amd0814-rockford-aerospace-infographic

Muhammad Aamir, Khaled Giasinb, Majid Tolouei-Rada, Ana Vafadar, A review: drilling performance and hole quality of aluminium alloys for aerospace applications, Journal of Materials Research and Technology. 2 0 2 0;9(6):12484–12500

Murat Sarikaya, Munish Kumar Gupta, Italo Tomaz, Mohd Danish, Mozammel Mia, Saeed Rubaiee, Mohd Jamil, Danil Yu Pimenov, Navneet Khanna, Cooling techniques to improve the machinability and sustainability of light-weight alloys: A state-of-the-art review, 179-201, 23, Journal of Manufacturing Processes, 62, Published - Feb 2021

Muthusamy, Y., Kadirgama, K., Rahman, M.M. et al. Wear analysis when machining AISI 304 with ethylene glycol/TIO2 nanoparticle-based coolant. Int J Adv Manuf Technol 82, 327–340 (2016). https://doi.org/10.1007/s00170-015-7360-3

N. Eswara Prasad Amol A. Gokhale R.J.H. Wanhill, Aluminum Lithium Alloys Processing, Properties, and Applications, 2014 Elsevier Inc.

N. Eswara Prasad, R.J.H. Wanhill, Aerospace Materials and Material Technologies, Volume 1: Aerospace Materials, Indian Institute of Metals Series. Springer Singapore, Chapter 24

N.S.M. Sahid1 , M.M. Rahman1 , K. Kadirgama1 , D. Ramasamy1 , M.A. Maleque2 and M.M. Noor1, Experimental investigation on the performance of the TiO2 and ZnO hybrid nanocoolant in ethylene glycol mixture towards AA6061-T6 machining, International Journal of Automotive and Mechanical Engineering ISSN: 2229-8649 (Print); ISSN: 2180-1606 (Online); Volume 14, Issue 1 pp. 3913-3926 March 2017 ©Universiti Malaysia Pahang Publishing DOI: https://doi.org/10.15282/ijame.14.1.2017.8.0318

New Light Alloys, AGARD Lecture Series No. 174", North Atlantic Treaty Organization Advisory Group for Aerospace Research and Development, 1990

Nihat Tosun1 and Mesut Huseyinoglu2 Effect of MQL on Surface Roughness in Milling of AA7075-T6 Materials and Manufacturing Processes, 25: 793–798, 2010 Copyright © Taylor & Francis Group, LLC ISSN: 1042-6914 print/1532-2475 online DOI: 10.1080/10426910903496821

P. Rambabu, N. Eswara Prasad, V.V. Kutumbarao and R.J.H. Wanhill, "Aluminium Alloys for Aerospace Applications", Springer, Aerospace Materials and Material Technologies, Indian Institute of Metals Series, DOI 10.1007/978-981-10-2134-3_2

R.J.H. Wanhill, Aerospace Applications Of Aluminium – Lithium Alloys chapter 15, DOI:10.1007/978-981-10-2134-3_2, In book: Aerospace Materials and Material Technologies (pp.29-52)

ROBERTO J. RIOJA and JOHN LIU, The Evolution of Al-Li Base Products for Aerospace, S. Kalyanam, A.J. Beaudoin, R.H. Dodds Jr, F. Barlat, Delamination cracking in advanced aluminum–lithium alloys-experimental and computational studies, Eng Fract Mech, 2009,76:2174–91.

S.F. Hamel, A parametric study of delaminations in an aluminum–lithium alloy, In: MS Thesis.

Champaign, University of Illinois at Urbana, 2010.
Stan Imbrogno, Sergio Rinaldi, Asier Gurruchaga Suarez, Pedro J. Arrazola, Domenico Umbrello, High Speed Machinability of the Aerospace Alloy AA7075 T6 Under Different Cooling Conditions, Proceedings of the 21st International ESAFORM Conference on Material Forming AIP Conf. Proc. 1960, 070013-1–070013-6; https://doi.org/10.1063/1.5034909 Published by AIP Publishing. 978-0-7354-1663-5
Thakur Paramjit Mahesh a, R. Rajesh b Optimal Selection of Process Parameters in CNC End Milling of Al 7075-T6 Aluminium Alloy Using a Taguchi-fuzzy Approach, Procedia Materials Science, Volume 5, 2014, Pages 2493-2502
Thomas Dorin, Alireza Vahid, Justin Lamb, "Fundamentals of Aluminium Metallurgy", Elsevier, DOI: 10.1016/B978-0-08-102063-0.00011-4
Thomas Dorin, Alireza Vahid, Justin Lamb, Fundamentals of Aluminum Metallurgy, 2018, B978-0-08-102063-0.00011-4 387
Ujjawal Kumar , Akshay Majumdar , V.K. Hiremath, Properties of Aluminum-Lithium Alloy – A New Aerospace Alloy, International Journal of Engineering & Technology Research Volume 3, Issue 3, May-June, 2015, pp. 29-35 ISSN Online: 2347-4904
V Muthuraman1 , and S Arunkumar Experimental evaluation of machining parameters in machining of 7075 aluminium alloy with cryogenic liquid nitrogen coolant, International Conference on Emerging Trends in Engineering Research IOP Conf. Series: Materials Science and Engineering 183 (2017) 012012 doi:10.1088/1757-899X/183/1/012012
Vasanth Kumar H S. (2022). Impact of Silicon Carbide Particles Weight Percentage on the Microstructure, Mechanical Behaviour, and Fractography of Al2014 Alloy Composites. Advances in Materials Science and Engineering, 2022, 1-10, https://doi.org/10.1155/2022/2839150.
Vincent Wagner, Arnaud Vissio, Emmannuel Duc, Michele Pijolat, " Relationship between Cutting Conditions and Chips morphology during milling of Aluminum Al-2050", Int. J Mnanuf. Technol (2016), 82:1881-1897
Vincent Wagner, Arnaud Vissio, Emmannuel Duc, Michele Pijolat, Relationship between Cutting Conditions and Chips morphology during milling of Aluminum Al-2050, Int. J Mnanuf. Technol (2016), 82:1881-1897
Volume 31, Issue 4, April 2010, Pages 1768-1775
Xuesong Zhang, Yongjun Chen, Junling Hu, "Recent advances in the development of aerospace materials", Progress in Aerospace Sciences 97, Elsevier (2018) 22–34
Yue Yang, Jing Bi, Hanwei Liu, Yang Li, Mingyang Li, Sansan Ao, Zhen Luo, "Research progress on the microstructure and mechanical properties of friction stir welded Al–Li alloy joints", Elsevier, Journal of Manufacturing Processes 82 (2022) 230-244, https://doi.org/10.1016/j.jmapro.2022.07.067
Zainul Huda, Prasetyo Edi, Materials selection in design of structures and engines of supersonic", Elsevier, Materials and Design 46 (2013) 552–560

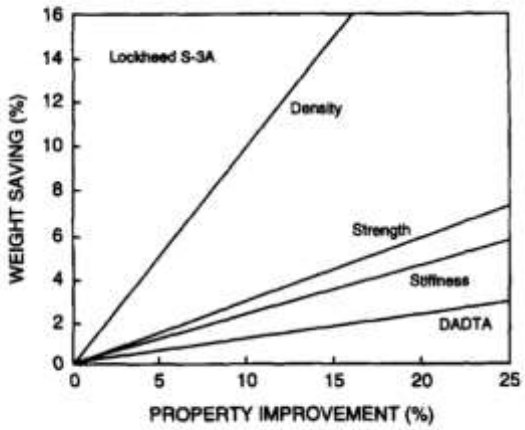

Fig 1: Graph weight savings and property improvement. [6]

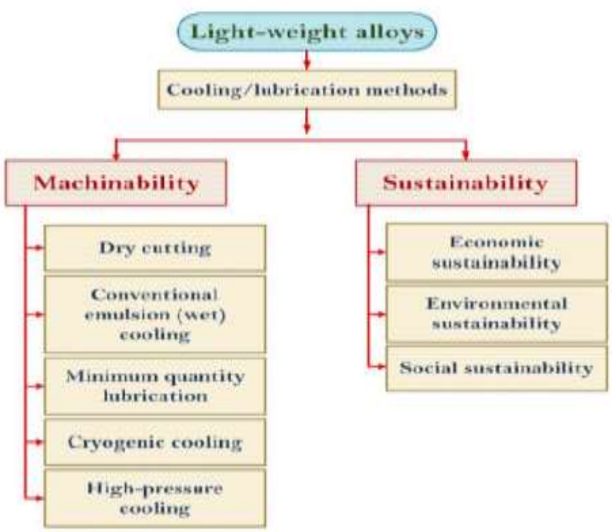

Fig 2: Coolant strategies and methods for light weight alloys [28].

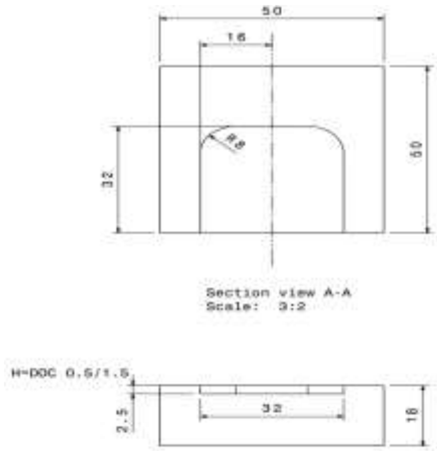

Fig.3: Sample specimen drawing of size 50 x 50 x 20 mm

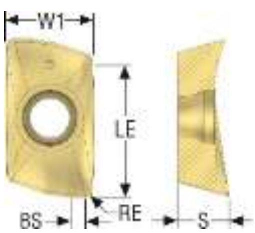

Fig.4: Seco Insert Carbide Uncoated from XOEX10T3

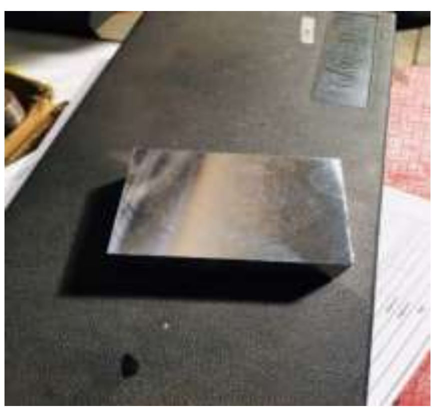

Fig: 5: Specimen Before machining

Fig. 6: Secimen After Machining

Fig. 7: Experimental set-up of the milling of a sample specimen

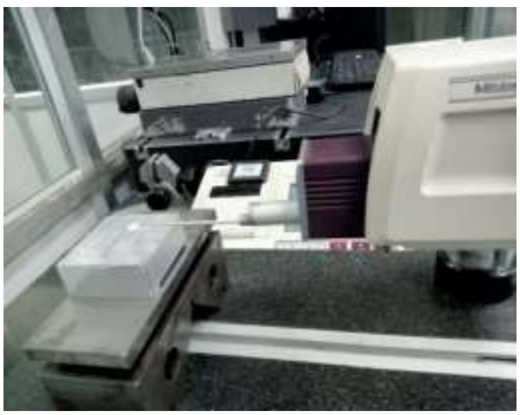

Surface roughness measurement using 410 Surf test on Sample specimen

HAZ measurment using Eddy current meter on Sample specimen

Fig 8: Testing of Ra and HAZ using 410 Surf-test and EDDY current meter

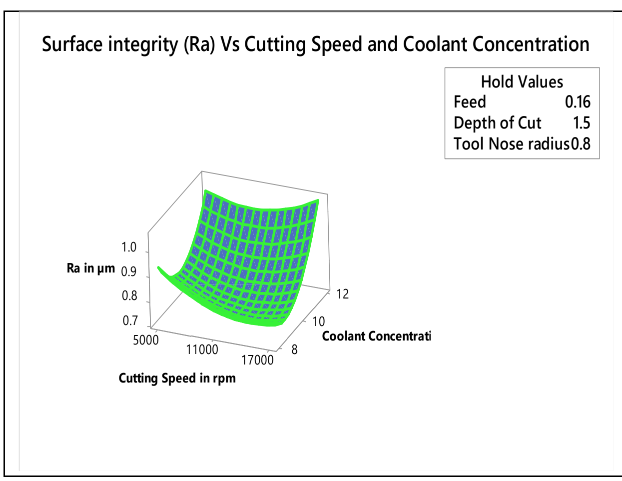

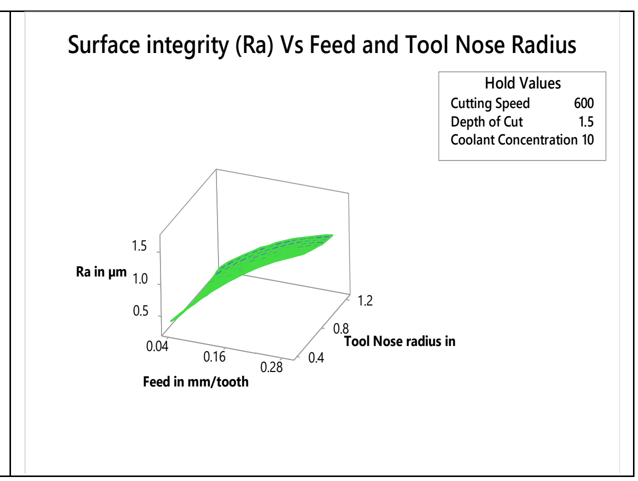

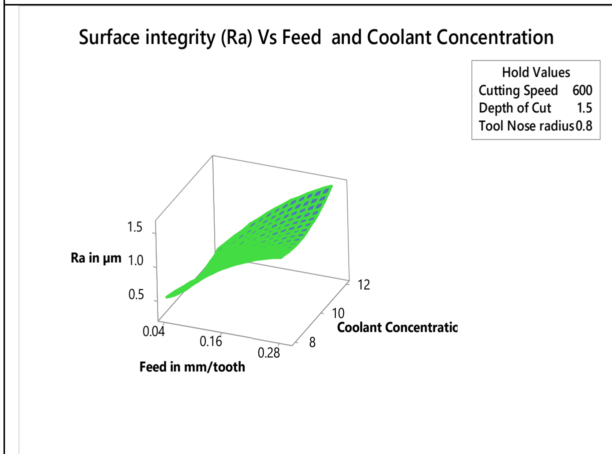

4.1 a.

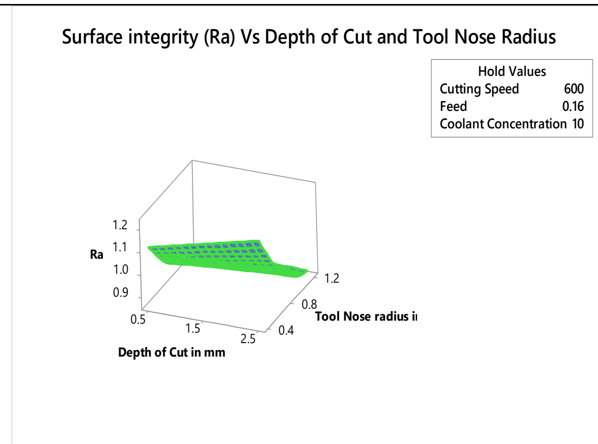

4.1.b

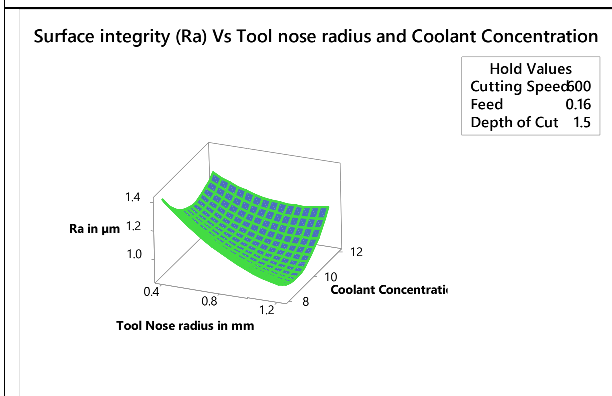

4.1.c

4.1.d

4.1.e

Fig: 4.1 a) Surface plot of CS and Coolant connetration b) Surface plot of Feed and Tool nose radius c) Surface plot of Feed and Coolant connetration d) Surface plot of Depth of Cut and Tool nose radius e) Surface plot of Tool nose radius and Coolant connetration

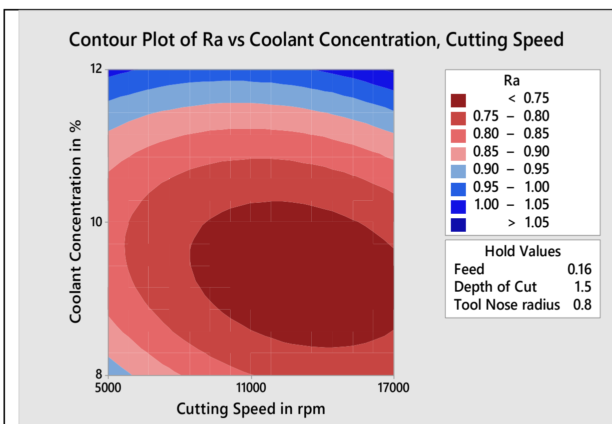

4.2.a

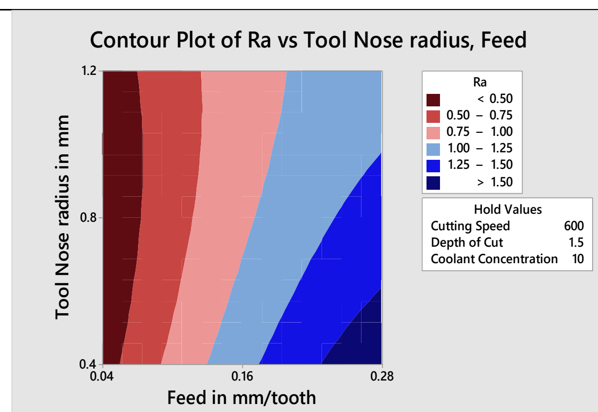

4.2.b Contour plots for Feed and Tool nose radius

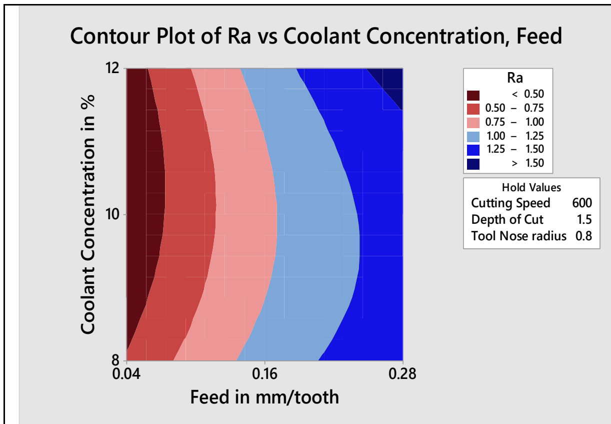

4.2.c

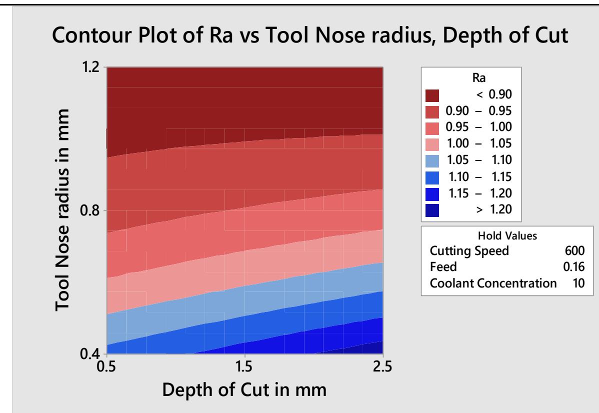

4.2.d

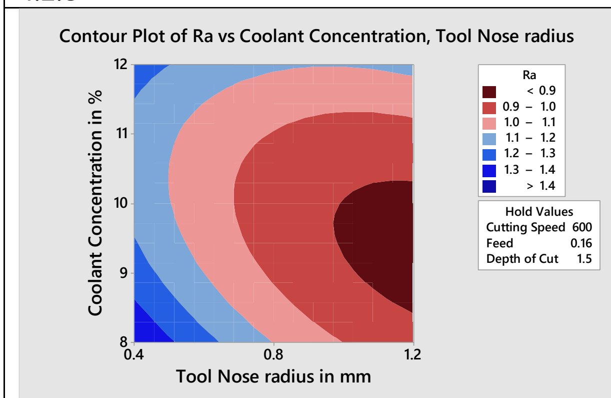

4.2.e

Fig: 4.2. a) Contour plots for Cutting speed and Coolant concentration b) Contour plots for Feed and Tool nose radius c) Contour plots for Feed and Coolant concentration d) Contour plots for Depth of cut and Tool Nose radius e) Contour plots for Coolant concentration and Tool nose radius

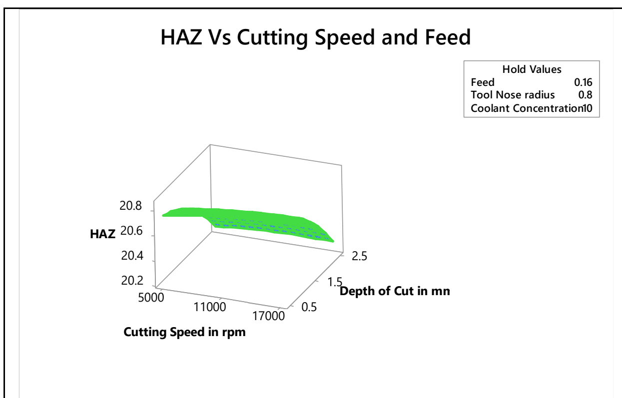

4.3.a

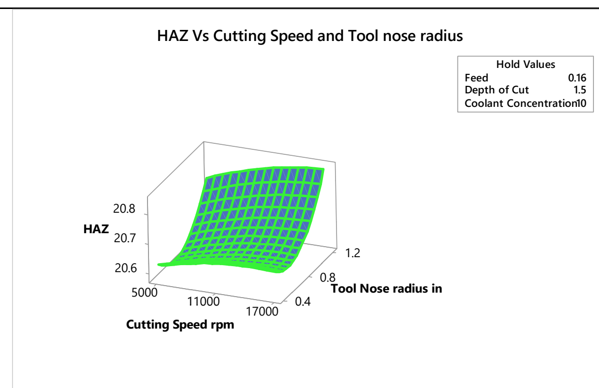

4.3.b

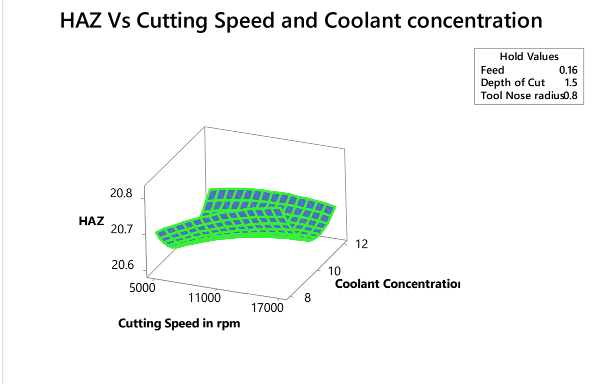

4.3.c

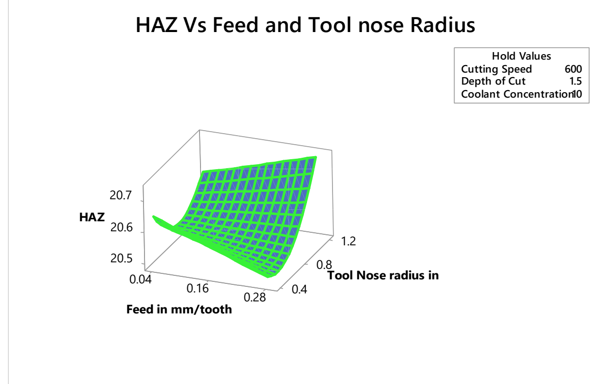

4.3.d

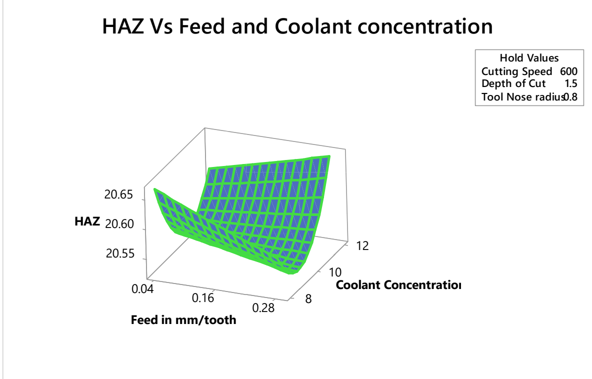

4.3.e

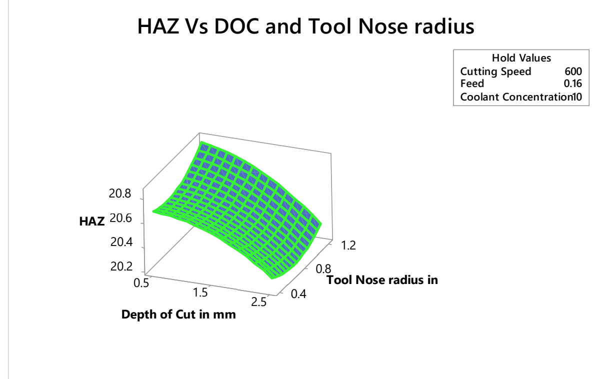

4.3.f

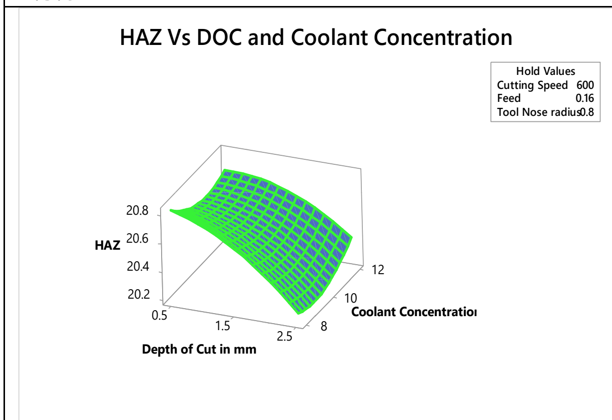

4.3.g

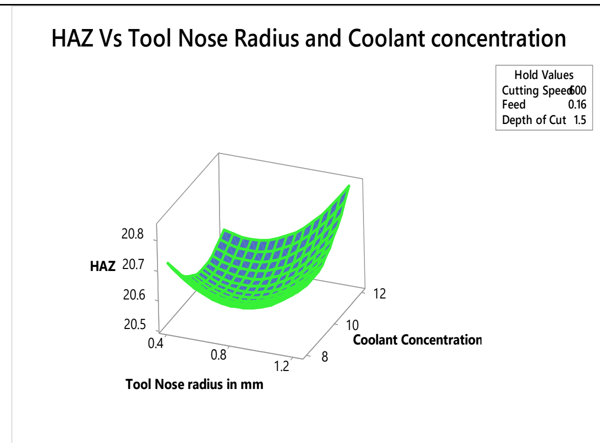

4.3.h

Fig: 4.3.a) Surface plot of Cutting speed and depth of cut, b) Surface plot of Cutting speed and tool nose radius, c) Surface plot of CS and Coolant concentration, d) Surface plot of Feed and Tool nose radius, e) : Interaction plot: Surface plot of CS and Coolant connetration, f) Surface plot of Feed and Tool nose radius, g) Surface plot of Depth of cut and Coolant connetration, h) Surface plot of Coolant concentration and Tool nose radius

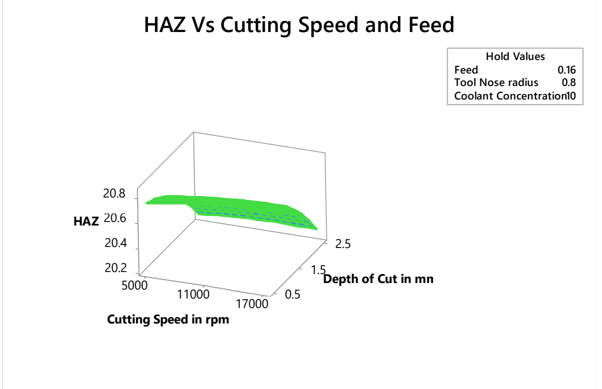

4.3.a

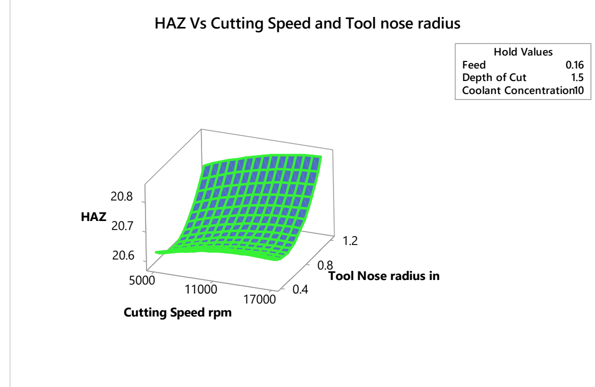

4.3.b

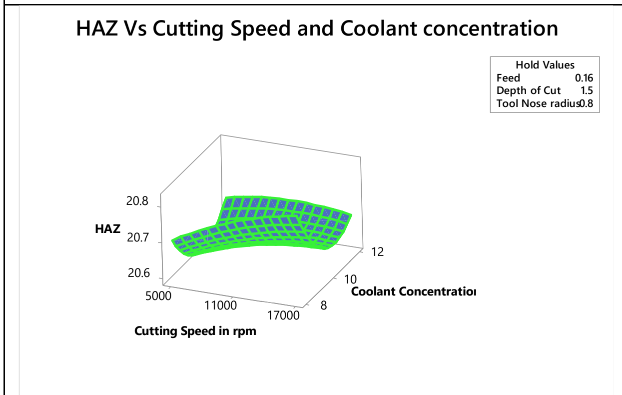

4.3.c

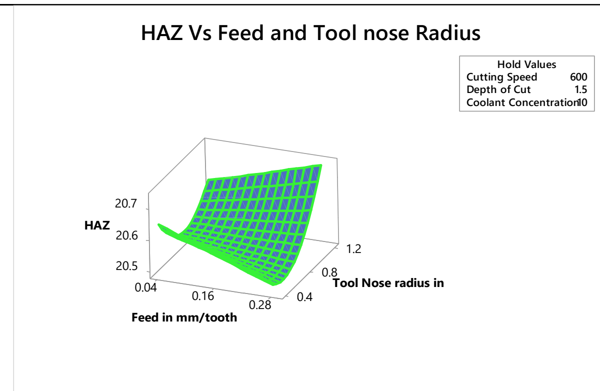

4.3.d

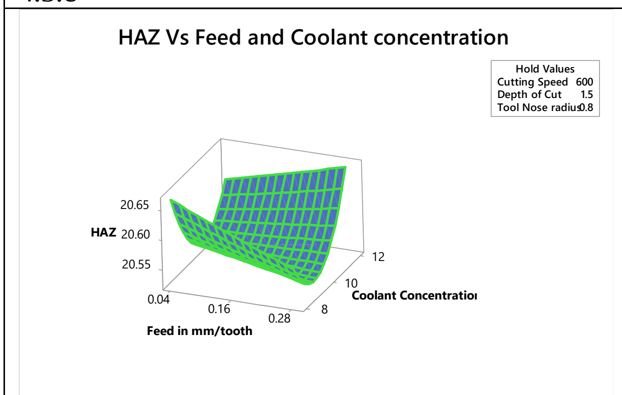

4.3.e

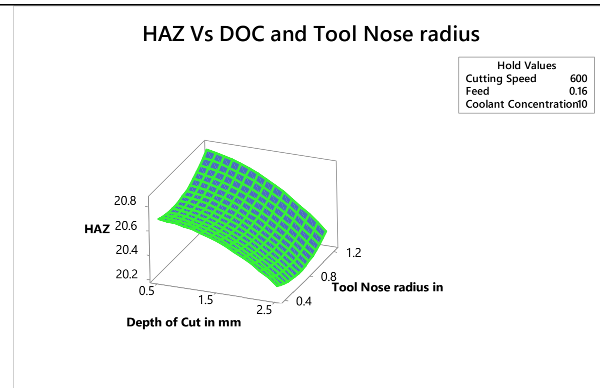

4.3.f

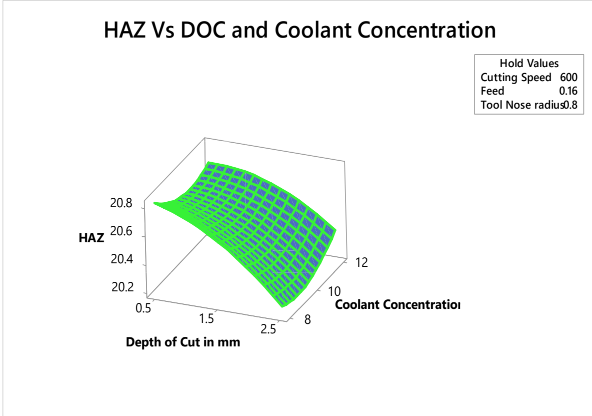

4.3.g

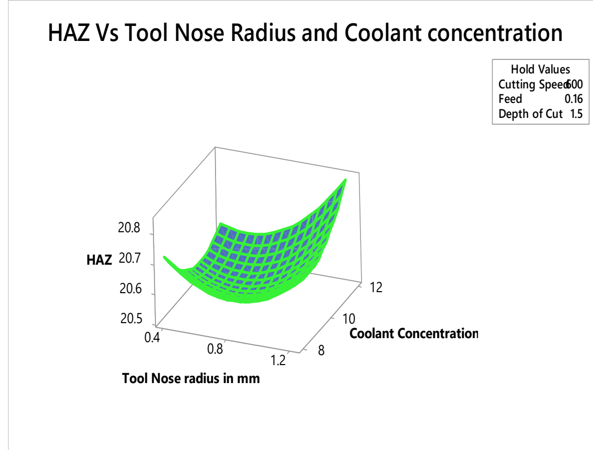

4.3.h

Fig: 4.3.a) Surface plot of Cutting speed and depth of cut, b) Surface plot of Cutting speed and tool nose radius, c) Surface plot of CS and Coolant concentration, d) Surface plot of Feed and Tool nose radius, e) : Interaction plot: Surface plot of CS and Coolant connetration, f) Surface plot of Feed and Tool nose radius, g) Surface plot of Depth of cut and Coolant connetration, h) Surface plot of Coolant concentration and Tool nose radius

Table.1: Chemical Composition of Al-Li alloys [11]

Al Li alloys	**Li**	**Cu**	**Zn**	**Mg**	**Mn**	**Fe**	**Si**	**Cr**	**Zr**	**Ti**	**Others**
2050	**0.7-1.3**	3.2-3.9	0.25	0.2-0.6	0.2-0.5	0.1	0.08	0.05	0.06-0.14	0.1	0.2-0.7 Ag
2090	**1.9-2.6**	2.4-30.0	0.1	0.25	0.05	0.12	0.1	0.05	0.08-0.15	0.15	
2098	**0.8-1.3**	3.2-3.8	0.35	0.25-0.8	0.35	0.15	0.12		0.04-0.18	0.1	0.25-0.6 Ag
2099	**1.6-2.0**	2.4-3.0	0.4-1.0	0.1-0.5	0.1-0.5	0.07	0.05	0.1-0.5	0.05-0.12	0.1	0.0001 Be
2199	**1.4-1.8**	2.0-2.9	2.0-0.9	0.05-0.4	0.1-0.5	0.07	0.05		0.05-0.12	0.1	0.0001 Be

Table 2: 7075 Aluminum Alloy 2nd generation material

Ref.	**Workpiece**	**Cutting Environment**	**Machining**	**Parameters evaluated Responses**	**Remarks**
31	AA7075	Dry, MQL Cryogenic	Turning	CF, Cutting Temperature, chip Morphology, Tool Wear	• Feed component affected by cooling techniques. • MQL and cryogenic led to lower temperature

					• Cooling techniques affected the lesser Tool wear
32	AA 7075-T6	Dry, MQL HPAJ, Cryogenic (LN2)(air, and vegetable oil emulsion)	Turning	Microstructure, Surface Roughness	• Analytical model for fatigue life prediction • cryogenic technique led to lower temperature
33	Al7075	Dry and Cutting fluid using Gate ECM 1	Drilling	Tool wear, Burr Measurement	• Cutting fluid resulted in lower tool wear • Cutting fluid resulted in 20%lower burr rate
34	Al 7075	Dry	Turning	MRR, SR, Cylindricity error, circularity error	• Optimization of multiple outputs • Increase in speed increased the CF also increase in SR and Circularity and cylindricity
35	Al 7075	Dry	Milling	Temperature,	• Behavior of different tool geometries and coatings
36	AA 7075	Dry, wet and cryogenic	Boring	SR, Temperature, Force	• Cryogenic leads to less Cutting force, temperature, Surface roughness • Direct application of coolant recommended
37	Al 7075 – T6	Dry, MQL, Cryogenic and Compressed air	Turning	Tool wear, SR, Micro hardness, Force, Chip Morphology	• MQL, RHVT, and Compressed air, for improvement in SR and Tool wear • Absence of Crater wear due to coolant conditions
38	Al 7075 – T6	Coolant not specified	Milling	SR,	• Nose radius and depth of cut significant for minimizing the Surface roughness
39	Al 7075	Wet and LN2	Turning	SR, Temperature, Force	• Use of LN2 reduced the temperature, forces and surface roughness •
40	Al 7075	MQL, Compressed Air	Milling	SR, MRR	• Speed and Feed rate was the important parameter that affected the SR

					• Less viscous the coolant is effective
41	Al 7075 – T6	Dry and MQL using Mecgreen 550 Lubricant	Turning	SR and Chip formation	• Chip formation is dependent on feed rate, CS and Lubricating conditions • SR mainly dependent on feed rate
42	Al 7136-T6511	Blastocut BC 35 SW	Milling	SR	• CS is the factor that Affects the SR.
43	Al 7075-T6	Nano Silver and Borax additives with 95% ethylene glycol (Suspension form)	Milling	SR, CF and Chip formation	• Tribological Performance of Borax and nano Silver added EG • Nano Silver particles will improve the SR and solution prepared with EG has an industrial usage.

Table 3: 3rd Generation Aluminum alloys

Ref.	Workpiece /Tool material	Cutting Environment	Machining	Parameters evaluated Responses	Remarks
44	AA2024-T3	Dry, Base Fluid (Mineral Oil) MQL, NFMQL MoS2	Turning	Surface Topography, Temperature	• Surface Roughness was better with NFMQL than dry and MQL because of MoS2 • BUE is less with NFMQL
45	AA2050	Soluble oil emulsion	Tapping	Machining Distortion MRR	• Optimization of Machining time • Low values of distortion from the geometrical tolerances
46	Al2050	Dry and WET Emulsion Quakercool 7000 ALF 8%	Milling	Chip Morphology	• CS assists in reducing the chip size • Reduction in rake angle reduces the chip thickness
47	2A 97	Dry	Milling	Chip Morphology, Ra	• Cutting Speed played an important role for chip edge • Convenient for replacing the Conventional Al alloys for aircrafts

48	Al 8112	Vegetable oil (Copra Oil) as base oil, nano fluid	Milling	MRR	• Increase in depth of cut increases the MRR • Helix angle plays an important role for improving the MRR
49	Aluminium alloy 24345	Dry	Milling	Ra and Rz	• Uncoated and polished flute cutters perform far better coated cutters • Rz and Sdr give a better picture of the actual surface from the functionality point of view
50	Al 2024-T3	Dry	Drilling	Hole Deviation and Circularity	• Burrs were less with uncoated drill bit • CS also the significant parameter for geometrical parameters

Table 4: Coolant as Ethylene Glycol

Ref.	**Workpiece**	**Cutting Environment**	**Machining**	**Parameters evaluated Responses**	**Remarks**
51	SUS 304	Cellulose nanocrystal ethylene glycol	Turning	Thermal Conductivity Analysis, cutting tool and chp thermal analysis,	• Thermal conductivity increases as concentration increases
52	AISI 1018	Ethylene glycol as base fluid, TiO2 and Al2O3 nanoparticles	Turning	Temperature, SR	• Thermal Analysis was studied along with SR
	Al 3303	Water ethylene glycol mixture		Corrosion study	• Corosion properties
53	AISI 304	Ethylene glycol TiO2 nano particles	Milling	Tool life, tool wear	• Tool ife decreases with increase increase in cutting speed • Showed better performance with water soluble coolants in terms of tool life.

54	AA6061-T6	Ethylene glycol mixture with TiO2 and ZnO hybrid nano coolant	Milling	SR, MRR	• Suitable alternative and compatible in using the hybrid nano-coolant
55	Fe3O4 nanofluid	Ehtylene glycol and waterbased mixture		Thermal Conductivity, Effect of temperture	• Thermal Conductivity enhancement

Table 5: Process parameters

Variables			Levels	
		-1	**0**	**1**
Cutting Speed(rpm)	X1	5000	11000	17000
Feed(mm/tooth)	X2	0.04	0.16	0.28
Depth of Cut(mm)	X3	0.5	1	1.5
Tool Nose Radius	X4	0.4	0.8	1.2
Coolant Concentration (%)	X5	8	10	12

Table 6: Physical properties of 3rd Generation

Cu	Li	Mg	Mn	Ag	Zr	Bal.
3.5	0.9	0.40	0.35	0.45	0.12	Re m.
SAE AMS4413B Solution Heat Treated, Stress Relieved, and Artificially Aged						

Table:7: Physical properties of 3rd Generation

Properties	Value
Density	270 gm/cc
Melting point	510 ° C
Tensile Strength	440 MPa
Yield Strength	370 MPa
Shear Strength	260 MPa

Fatigue Strength	125
Elastic Modulus	70-80 GPa
Poison's Ratio	0.33
Elongation	10%

Table. 8: Coolant Details: Specifications of Ethylene Glycol: MOLYCHEM

Ethylene Glycol	1,2 Ethanediol
Ethylene Glycol	98%
Molecular formula	$C_2H_6O_2$
Color	A clear colorless, slightly viscous liquid
Wt. per ML at 20°C	1.112-1.115g

Table 4.1: ANOVA (Ra)

Source Ra	**Un-Coded Values**	**DF**	**Adj SS**	**Adj MS F-Value**	**F-Value**	**P value**	**Significant Factors**
Model		20	37.69580	1.88480	13.70000	0.00000	
Linear		5	33.27930	6.65590	479.20000	0.00000	
Cutting Speed	X1	1	0.06440	0.06440	4.63000	0.13800	
Feed	X2	1	31.11960	31.11960	2240.51000	0.00000	*
Depth of Cut	X3	1	0.00880	0.00880	0.63000	0.35800	
Tool Nose Radius	X4	1	1.26500	1.26500	91.07000	0.00000	*
Coolant Concentration	X5	1	0.82170	0.82170	59.16000	0.67600	
Square		5	1.00750	0.20150	14.51000	0.00000	*
Cutting Speed * Cutting Speed	$X1^2$	1	0.02450	0.02450	1.76000	0.18600	
Feed * Feed	$X2^2$	1	0.12530	0.12530	0.02000	0.00300	*
DOC * DOC	$X3^2$	1	0.00000	0.00000	0.00000	0.99900	
Tool Nose radius*Tool Nose radius	$X4^2$	1	0.04020	0.04020	2.90000	0.09100	
Coolant Concentration*Coolant Concentration	$X5^3$	1	0.17500	0.17750	12.78000	0.00000	*
2-Way Interaction		10	3.40900	0.34090	24.54000	0.00000	
Cutting Speed*Feed	X1 * X2	1	0.01360	0.01360	0.98000	0.32400	
Cutting Speed*Depth of Cut	X1 * X3	1	0.00520	0.00520	0.38000	0.54100	
Cutting Speed*Tool Nose radius	X1 * X4	1	0.03700	0.03700	2.66000	0.10500	
Cutting Speed*Coolant	X1 * X5	1	0.20310	0.02031	14.63000	0.00000	*

Concentration							
Feed*Depth of Cut	X2 * X3	1	0.08780	0.08780	6.32000	0.01300	
Feed*Tool Nose radius	X2 * X4	1	1.46420	1.46420	105.42000	0.00000	*
Feed*Coolant Concentration	X2 * X5	1	0.73640	0.73640	53.02000	0.00000	*
Depth of Cut*Tool Nose radius	X3 * X4	1	0.11500	0.11500	8.28000	0.00000	*
Depth of Cut*Coolant Concentration	X3 * X5	1	0.00000	0.00000	0.00000	0.96000	
Tool Nose radius*Coolant Concentration	X4 * X5	1	0.74660	0.74660	53.75000	0.00000	*

Table 4.2 : ANOVA (HAZ)

Source HAZ	Un-Coded Values	DF	Adj SS	Adj MS F-Value	F-Value	P value	Significant Factors
Model		20	9.62100	0.48060	143.51000	0.00000	
Linear		5	7.87910	1.57583	470.55000	0.00000	
Cutting Speed	X1	1	0.04055	0.10547	31.50000	0.00000	
Feed	X2	1	0.02100	0.02104	6.28000	0.01300	*
Depth of Cut	X3	1	6.93690	6.93686	2071.40000	0.00000	
Tool Nose Radius	X4	1	0.62510	0.62510	186.66000	0.00000	*
Coolant Concentration	X5	1	0.19070	0.19067	56.93000	0.00000	*
Square		5	0.33000	0.06739	20.12000	0.00000	*
Cutting Speed * Cutting Speed	$X1^2$	1	0.00230	0.00229	0.68000	0.40900	
Feed * Feed	$X2^2$	1	0.00000	0.00002	0.01000	0.94000	*
DOC * DOC	$X3^2$	1	0.06140	0.06137	18.33000	0.00000	*
Tool Nose radius*Tool Nose radius	$X4^2$	1	0.06460	0.06460	19.29000	0.00000	*
Coolant Concentration* Coolant Concentration	$X5^3$	1	0.06350	0.06345	18.95000	0.00000	*
2-Way Interaction		10	1.39600	0.13960	41.68000	0.00000	*
Cutting Speed*Feed	X1 * X2	1	0.00140	0.00139	0.41000	0.52100	
Cutting Speed*Depth of Cut	X1 * X3	1	0.03470	0.03469	10.36000	0.00200	*
Cutting Speed*Tool Nose radius	X1 * X4	1	0.01880	0.01884	5.63000	0.01900	
Cutting Speed*Coolant Concentration	X1 * X5	1	0.08140	0.08138	24.30000	0.00000	*
Feed*Depth of Cut	X2 * X3	1	0.00310	0.00309	0.92000	0.33800	
Feed*Tool Nose radius	X2 * X4	1	0.34980	0.34981	104.46000	0.00000	*
Feed*Coolant Concentration	X2 * X5	1	0.11310	0.11309	104.46000	0.00000	*

Depth of Cut*Tool Nose radius	X3 * X4	1	0.113 10	0.11309	33.77000	0.0000 0	*
Depth of Cut*Coolant Concentration	X3 * X5	1	0.389 50	0.38951	116.3100 0	0.0000 0	*
Tool Nose radius*Coolant Concentration	X4 * X5	1	0.308 80	0.30883	92.22000	0.0000 0	*